Artificial Intelligence for Sustainable Development: Optimizing Land Cover for India's Growing Population

Forrest M. Hoffman
forrest@climatemodeling.org

Oak Ridge National Laboratory and University of Tennessee

Department of Development Studies & Agri Business Management Seminar

Vivekananda Global University (VGU)

February 4, 2025

Forrest M. Hoffman, Computational Earth System Scientist

- Group Leader for the ORNL Computational Earth Sciences Group
- 36 years at ORNL in Environmental Sciences Division, then Computer Science and Mathematics Division, and now Computational Sciences and Engineering Division
- Develop and apply Earth system models to study global biogeochemical cycles, including terrestrial & marine carbon cycle
- Investigate methods for reconciling uncertainties in carbon–climate feedbacks through comparison with observations
- Apply artificial intelligence methods (machine learning and data mining) to environmental characterization, simulation, & analysis
- Joint Faculty, University of Tennessee, Knoxville, Department of Civil & Environmental Engineering

OAK RIDGE National Laboratory

THE UNIVERSITY OF TENNESSEE KNOXVILLE

Introduction

- **Sustainable Development across Landscapes** requires understanding of
  - What constitutes sustainability & resilience in the context of climate change
  - Community dynamics, population, and societal needs
  - Global Earth system dynamics and feedbacks to the carbon cycle
  - Regional to local environmental science and responses to climate change
  - Geographic characterization of human systems, ecosystems, and their interactions across space and time scales in global landscapes
- We must be able to apply **advanced technologies** to
  - Characterize environmental conditions and monitor change
  - Model the interactive dynamics of Earth system components
  - Perform model-data integration for sophisticated analysis of Big Data
  - Develop new understanding of Earth system processes

Introduction

- Observations of the Earth system are increasing in spatial resolution and temporal frequency, and will grow exponentially over the next 5–10 years
- With Exascale computing, simulation output is growing even faster, outpacing our ability to analyze, interpret and evaluate model results
- Explosive data growth and the promise of discovery through data-driven modeling necessitate new methods for feature extraction, change/anomaly detection, data assimilation, simulation, and analysis

Frontier at Oak Ridge National Laboratory is the #2 fastest supercomputer on the TOP500 List and the first supercomputer to break the exaflop barrier (Nov 18, 2024).

This article is the second in a two-part series. The first part, "How to Build a Hypercomputer," by Thomas Sterling, appeared in the July 2001 issue.

The Do-It-Yourself

Supercomputer

By William W. Hargrove, Forrest M. Hoffman and Thomas Sterling

Photographs by Kay Chernush

Scientists have found a cheaper way to solve tremendously difficult computational problems: connect ordinary PCs so that they can work together

CLUSTER OF PCs at the Oak Ridge National Laboratory in Tennessee has been dubbed the Stone SouperComputer.

Copyright 2001 Scientific American, Inc.

Multivariate Geographic Clustering

- Ecoregions have traditionally been created by experts
- Our approach has been to objectively create ecoregions using continuous continental-scale data and clustering
- We developed a highly scalable *k*-means cluster analysis code that uses distributed memory parallelism
- Originally developed on a 486/Pentium cluster, the code now runs on the largest hybrid CPU/GPU architectures on Earth

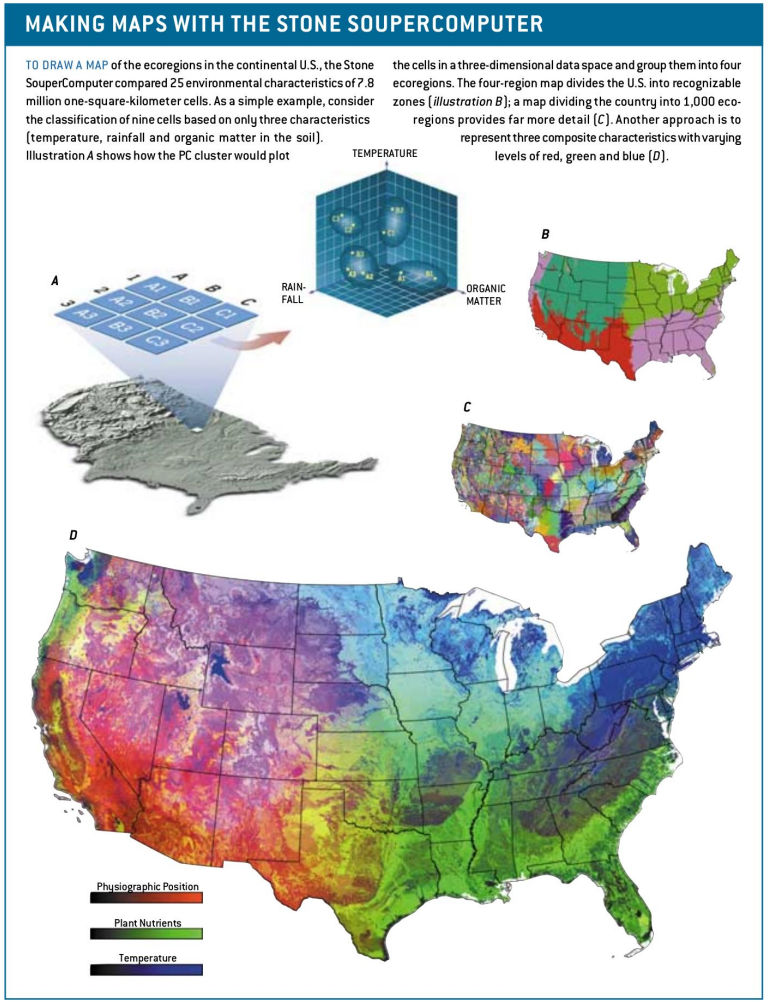

Hargrove, W. W., F. M. Hoffman, and T. Sterling (2001), The Do-It-Yourself Supercomputer, *Sci. Am.*, 265(2):72–79, https://www.scientificamerican.com/article/the-do-it-yourself-superc/

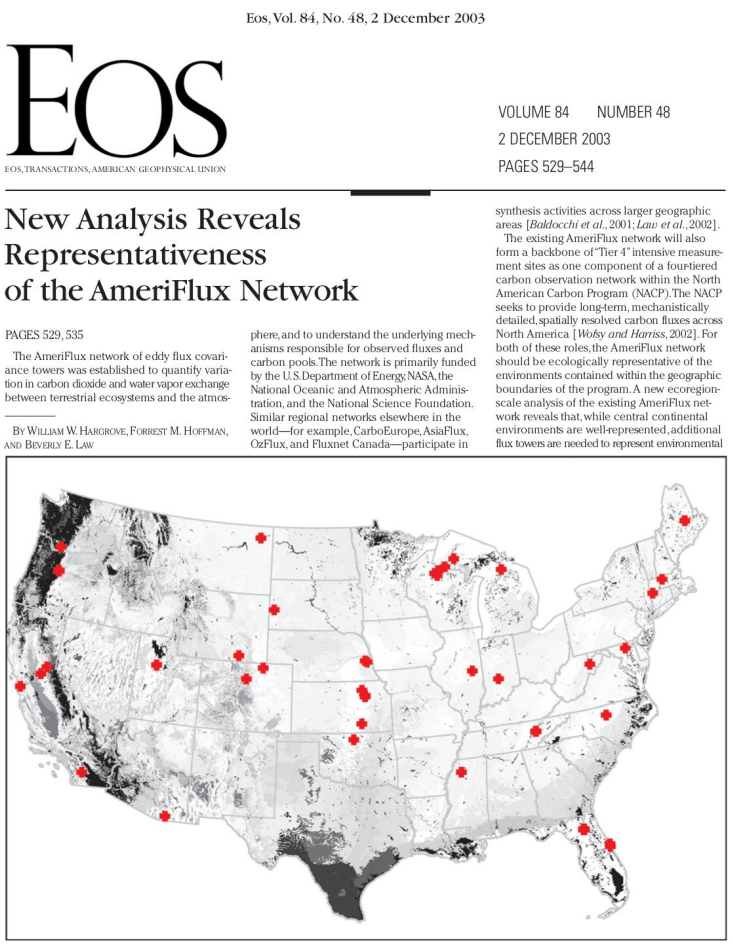

Eos, Vol. 84, No. 48, 2 December 2003

EOS

EOS, TRANSACTIONS, AMERICAN GEOPHYSICAL UNION

VOLUME 84 NUMBER 48
2 DECEMBER 2003
PAGES 529–544

New Analysis Reveals Representativeness of the AmeriFlux Network

PAGES 529, 535

The AmeriFlux network of eddy flux covariance towers was established to quantify variation in carbon dioxide and water vapor exchange between terrestrial ecosystems and the atmosphere, and to understand the underlying mechanisms responsible for observed fluxes and carbon pools. The network is primarily funded by the U.S. Department of Energy, NASA, the National Oceanic and Atmospheric Administration, and the National Science Foundation. Similar regional networks elsewhere in the world—for example, CarboEurope, AsiaFlux, OzFlux, and Fluxnet Canada—participate in synthesis activities across larger geographic areas [*Baldocchi et al.*, 2001; *Law et al.*, 2002].

The existing AmeriFlux network will also form a backbone of "Tier 4" intensive measurement sites as one component of a four-tiered carbon observation network within the North American Carbon Program (NACP). The NACP seeks to provide long-term, mechanistically detailed, spatially resolved carbon fluxes across North America [*Wofsy and Harriss*, 2002]. For both of these roles, the AmeriFlux network should be ecologically representative of the environments contained within the geographic boundaries of the program. A new ecoregion-scale analysis of the existing AmeriFlux network reveals that, while central continental environments are well-represented, additional flux towers are needed to represent environmental

By William W. Hargrove, Forrest M. Hoffman, and Beverly E. Law

Fig. 1. The representativeness of an existing spatial array of sample locations or study sites—for example, the AmeriFlux network of carbon dioxide eddy flux covariance towers—can be mapped relative to a set of quantitative ecoregions, suggesting locations for additional samples or sites. Distance in data space to the closest ecoregion containing a site quantifies how well an existing network represents each ecoregion in the map. Environments in darker ecoregions are poorly represented by this network.

Network Representativeness

- The *n*-dimensional space formed by the data layers offers a natural framework for estimating representativeness of individual sampling sites
- The Euclidean distance between individual sites in data space is a metric of similarity or dissimilarity
- Representativeness across multiple sampling sites can be combined to produce a map of network representativeness

Hargrove, W. W., and F. M. Hoffman (2003), New Analysis Reveals Representativeness of the AmeriFlux Network, *Eos Trans. AGU*, 84(48):529, 535, doi:10.1029/2003EO480001.

Optimizing Sampling Networks

- Our group produced this network representativeness map for the authors from global climate, edaphic, and elevation and topography data
- Dark areas, including most of the Indian subcontinent, were poorly represented by the constellation of eddy covariance flux towers participating in FLUXNET in the year 2007

Sundareshwar, P. V., et al. (2007), Environmental Monitoring Network for India, *Science*, 316(5822):204–205, doi:10.1126/science.1137417.

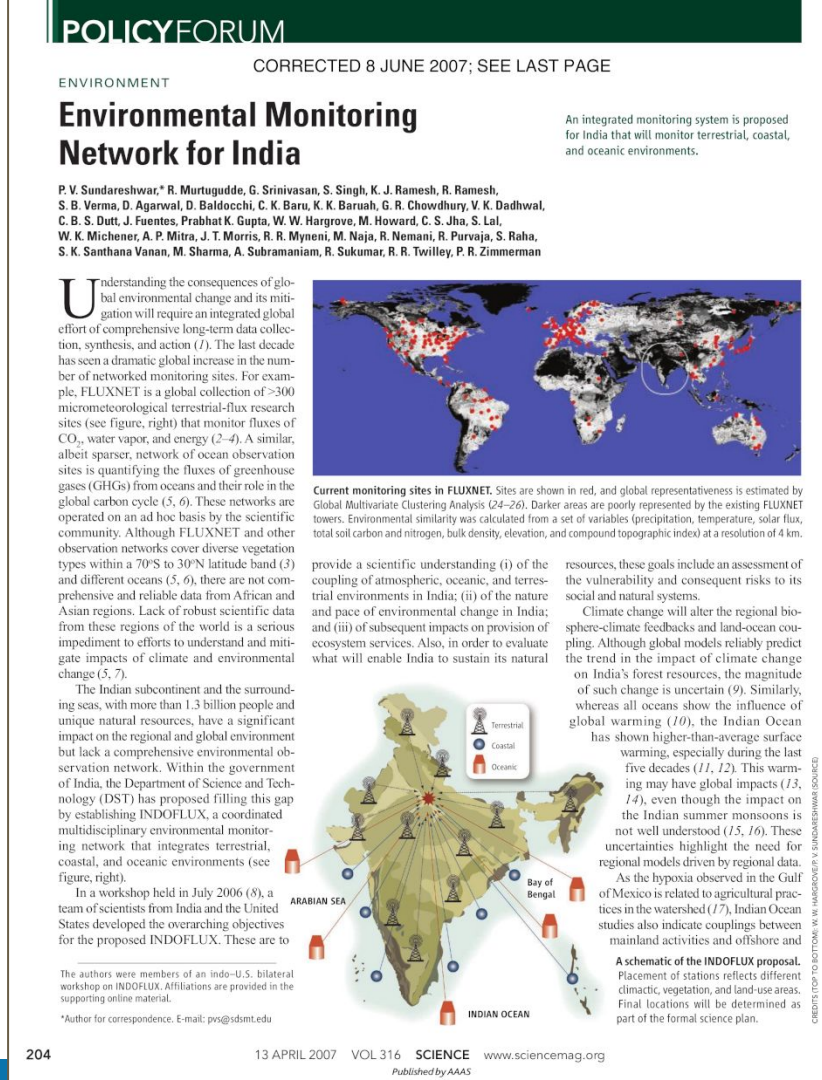

POLICYFORUM

CORRECTED 8 JUNE 2007; SEE LAST PAGE

ENVIRONMENT

Environmental Monitoring Network for India

An integrated monitoring system is proposed for India that will monitor terrestrial, coastal, and oceanic environments.

P. V. Sundareshwar,* R. Murtugudde, G. Srinivasan, S. Singh, K. J. Ramesh, R. Ramesh, S. B. Verma, D. Agarwal, D. Baldocchi, C. K. Baru, K. K. Baruah, G. R. Chowdhury, V. K. Dadhwal, C. B. S. Dutt, J. Fuentes, Prabhat K. Gupta, W. W. Hargrove, M. Howard, C. S. Jha, S. Lal, W. K. Michener, A. P. Mitra, J. T. Morris, R. R. Myneni, M. Naja, R. Nemani, R. Purvaja, S. Raha, S. K. Santhana Vanan, M. Sharma, A. Subramaniam, R. Sukumar, R. R. Twilley, P. R. Zimmerman

Understanding the consequences of global environmental change and its mitigation will require an integrated global effort of comprehensive long-term data collection, synthesis, and action (*1*). The last decade has seen a dramatic global increase in the number of networked monitoring sites. For example, FLUXNET is a global collection of >300 micrometeorological terrestrial-flux research sites (see figure, right) that monitor fluxes of CO_2, water vapor, and energy (*2*–*4*). A similar, albeit sparser, network of ocean observation sites is quantifying the fluxes of greenhouse gases (GHGs) from oceans and their role in the global carbon cycle (*5*, *6*). These networks are operated on an ad hoc basis by the scientific community. Although FLUXNET and other observation networks cover diverse vegetation types within a 70°S to 30°N latitude band (*3*) and different oceans (*5*, *6*), there are not comprehensive and reliable data from African and Asian regions. Lack of robust scientific data from these regions of the world is a serious impediment to efforts to understand and mitigate impacts of climate and environmental change (*5*, *7*).

The Indian subcontinent and the surrounding seas, with more than 1.3 billion people and unique natural resources, have a significant impact on the regional and global environment but lack a comprehensive environmental observation network. Within the government of India, the Department of Science and Technology (DST) has proposed filling this gap by establishing INDOFLUX, a coordinated multidisciplinary environmental monitoring network that integrates terrestrial, coastal, and oceanic environments (see figure, right).

In a workshop held in July 2006 (*8*), a team of scientists from India and the United States developed the overarching objectives for the proposed INDOFLUX. These are to provide a scientific understanding (i) of the coupling of atmospheric, oceanic, and terrestrial environments in India; (ii) of the nature and pace of environmental change in India; and (iii) of subsequent impacts on provision of ecosystem services. Also, in order to evaluate what will enable India to sustain its natural resources, these goals include an assessment of the vulnerability and consequent risks to its social and natural systems.

Climate change will alter the regional biosphere-climate feedbacks and land-ocean coupling. Although global models reliably predict the trend in the impact of climate change on India's forest resources, the magnitude of such change is uncertain (*9*). Similarly, whereas all oceans show the influence of global warming (*10*), the Indian Ocean has shown higher-than-average surface warming, especially during the last five decades (*11*, *12*). This warming may have global impacts (*13*, *14*), even though the impact on the Indian summer monsoons is not well understood (*15*, *16*). These uncertainties highlight the need for regional models driven by regional data.

As the hypoxia observed in the Gulf of Mexico is related to agricultural practices in the watershed (*17*), Indian Ocean studies also indicate couplings between mainland activities and offshore and

The authors were members of an indo–U.S. bilateral workshop on INDOFLUX. Affiliations are provided in the supporting online material.

*Author for correspondence. E-mail: pvs@sdsmt.edu

Current monitoring sites in FLUXNET. Sites are shown in red, and global representativeness is estimated by Global Multivariate Clustering Analysis (*24*–*26*). Darker areas are poorly represented by the existing FLUXNET towers. Environmental similarity was calculated from a set of variables (precipitation, temperature, solar flux, total soil carbon and nitrogen, bulk density, elevation, and compound topographic index) at a resolution of 4 km.

A schematic of the INDOFLUX proposal. Placement of stations reflects different climactic, vegetation, and land-use areas. Final locations will be determined as part of the formal science plan.

CREDITS (TOP TO BOTTOM): W. W. HARGROVE/P. V. SUNDARESHWAR (SOURCE)

Published by AAAS

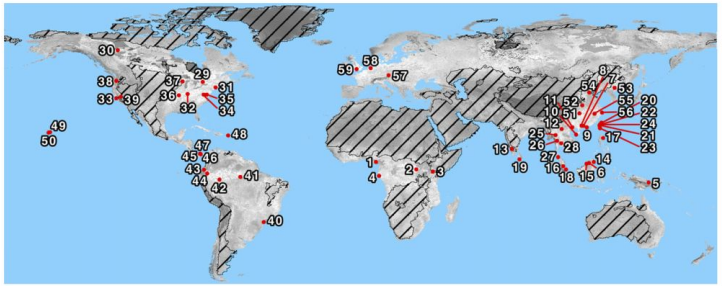

Fig. 1 Map of the CTFS-ForestGEO network illustrating its representation of bioclimatic, edaphic, and topographic conditions globally. Site numbers correspond to ID# in Table 2. Shading indicates how well the network of sites represents the suite of environmental factors included in the analysis; light-colored areas are well-represented by the network, while dark colored areas are poorly represented. Stippling covers nonforest areas. The analysis is described in Appendix S1.

Table 1 Attributes of a CTFS-ForestGEO census

Attribute	Utility
Very large plot size	Resolve community and population dynamics of highly diverse forests with many rare species with sufficient sample sizes (Losos & Leigh, 2004; Condit *et al.*, 2006); quantify spatial patterns at multiple scales (Condit *et al.*, 2000; Wiegand *et al.*, 2007a,b; Detto & Muller-Landau, 2013; Lutz *et al.*, 2013); characterize gap dynamics (Feeley *et al.*, 2007b); calibrate and validate remote sensing and models, particularly those with large spatial grain (Mascaro *et al.*, 2011; Réjou-Méchain *et al.*, 2014)
Includes every freestanding woody stem ≥1 cm DBH	Characterize the abundance and diversity of understory as well as canopy trees; quantify the demography of juveniles (Condit, 2000; Muller-Landau *et al.*, 2006a,b).
All individuals identified to species	Characterize patterns of diversity, species-area, and abundance distributions (Hubbell, 1979, 2001; He & Legendre, 2002; Condit *et al.*, 2005; John *et al.*, 2007; Shen *et al.*, 2009; He & Hubbell, 2011; Wang *et al.*, 2011; Cheng *et al.*, 2012); test theories of competition and coexistence (Brown *et al.*, 2013); describe poorly known plant species (Gereau & Kenfack, 2000; Davies, 2001; Davies *et al.*, 2001; Sonké *et al.*, 2002; Kenfack *et al.*, 2004, 2006)
Diameter measured on all stems	Characterize size-abundance distributions (Muller-Landau *et al.*, 2006b; Lai *et al.*, 2013; Lutz *et al.*, 2013); combine with allometries to estimate whole-ecosystem properties such as biomass (Chave *et al.*, 2008; Valencia *et al.*, 2009; Lin *et al.*, 2012; Ngo *et al.*, 2013; Muller-Landau *et al.*, 2014)
Mapping of all stems and fine-scale topography	Characterize the spatial pattern of populations (Condit, 2000); conduct spatially explicit analyses of neighborhood influences (Condit *et al.*, 1992; Hubbell *et al.*, 2001; Uriarte *et al.*, 2004, 2005; Rüger *et al.*, 2011, 2012; Lutz *et al.*, 2014); characterize microhabitat specificity and controls on demography, biomass, etc. (Harms *et al.*, 2001; Valencia *et al.*, 2004; Chuyong *et al.*, 2011); align on the ground and remote sensing measurements (Asner *et al.*, 2011; Mascaro *et al.*, 2011).
Census typically repeated every 5 years	Characterize demographic rates and changes therein (Russo *et al.*, 2005; Muller-Landau *et al.*, 2006a,b; Feeley *et al.*, 2007a; Lai *et al.*, 2013; Stephenson *et al.*, 2014); characterize changes in community composition (Losos & Leigh, 2004; Chave *et al.*, 2008; Feeley *et al.*, 2011; Swenson *et al.*, 2012; Chisholm *et al.*, 2014); characterize changes in biomass or productivity (Chave *et al.*, 2008; Banin *et al.*, 2014; Muller-Landau *et al.*, 2014)

Optimizing Sampling Networks

- The CTFS-ForestGEO global forest monitoring network is aimed at characterizing forest responses to global change
- The figure at left shows the global representativeness of the CTFS-ForestGEO sites in 2014
- Non-forested areas are masked with hatching, and as expected, they are consistently darker than the forested regions, which are represented to varying degrees by the monitoring sites

Anderson-Teixeira, K. J., et al. (2015), CTFS-ForestGEO: A Worldwide Network Monitoring Forests in an Era of Global Change, *Glob. Change Biol.*, 21(2):528–549, doi:10.1111/gcb.12712.

Representativeness for Alaska

Data Layers

Table: 37 characteristics averaged for the present (2000–2009) and the future (2090–2099).

Description	Number/Name	Units	Source
Monthly mean air temperature	12	°C	GCM
Monthly mean precipitation	12	mm	GCM
Day of freeze	mean	day of year	GCM
	standard deviation	days	
Day of thaw	mean	day of year	GCM
	standard deviation	days	
Length of growing season	mean	days	GCM
	standard deviation	days	
Maximum active layer thickness	1	m	GIPL
Warming effect of snow	1	°C	GIPL
Mean annual ground temperature at bottom of active layer	1	°C	GIPL
Mean annual ground surface temperature	1	°C	GIPL
Thermal offset	1	°C	GIPL
Limnicity	1	%	NHD
Elevation	1	m	SRTM

Hoffman, F. M., J. Kumar, R. T. Mills, and W. W. Hargrove (2013), Representativeness-Based Sampling Network Design for the State of Alaska, *Landscape Ecol.*, 28(8):1567–1586, doi:10.1007/s10980-013-9902-0.

Landscape Ecol (2013) 28:1567–1586
DOI 10.1007/s10980-013-9902-0

RESEARCH ARTICLE

Representativeness-based sampling network design for the State of Alaska

Forrest M. Hoffman · Jitendra Kumar · Richard T. Mills · William W. Hargrove

Received: 13 February 2013 / Accepted: 31 May 2013 / Published online: 20 June 2013

Abstract Resource and logistical constraints limit the frequency and extent of environmental observations, particularly in the Arctic, necessitating the development of a systematic sampling strategy to maximize coverage and objectively represent environmental variability at desired scales. A quantitative methodology for stratifying sampling domains, informing site selection, and determining the representativeness of measurement sites and networks is described here. Multivariate spatiotemporal clustering was applied to down-scaled general circulation model results and data for the State of Alaska at 4 km^2 resolution to define multiple sets of ecoregions across two decadal time periods. Maps of ecoregions for the present (2000–2009) and future (2090–2099) were produced, showing how combinations of 37 characteristics are distributed and how they may shift in the future. Representative sampling locations are identified on present and future ecoregion maps. A representativeness metric was developed, and representativeness maps for eight candidate sampling locations were produced. This metric was used to characterize the environmental similarity of each site. This analysis provides model-inspired insights into optimal sampling strategies, offers a framework for up-scaling measurements, and provides a down-scaling approach for integration of models and measurements. These techniques can be applied at different spatial and temporal scales to meet the needs of individual measurement campaigns.

Keywords Ecoregions · Representativeness · Network design · Cluster analysis · Alaska · Permafrost

F. M. Hoffman (✉)
Computer Science & Mathematics Division, Climate Change Science Institute (CCSI), Oak Ridge National Laboratory, Oak Ridge, TN, USA
e-mail: forrest@climatemodeling.org

F. M. Hoffman · J. Kumar · R. T. Mills
Environmental Sciences Division, Climate Change Science Institute (CCSI), Oak Ridge National Laboratory, Oak Ridge, TN, USA
e-mail: jkumar@climatemodeling.org

R. T. Mills
e-mail: rmills@ornl.gov

W. W. Hargrove
Eastern Forest Environmental Threat Assessment Center, USDA Forest Service, Southern Research Station, Asheville, NC, USA
e-mail: hnw@geobabble.org

Introduction

The Arctic contains vast amounts of frozen water in the form of sea ice, snow, glaciers, and permafrost. Extended areas of permafrost in the Arctic contain soil organic carbon that is equivalent to twice the size of the atmospheric carbon pool, and this large stabilized

10 Alaska Ecoregions, Present and Future

(Hoffman et al., 2013)

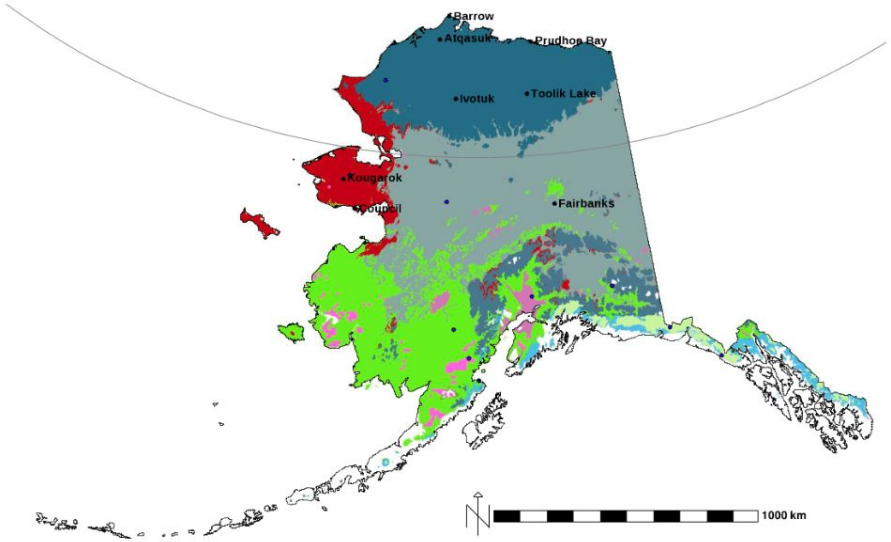

2000–2009

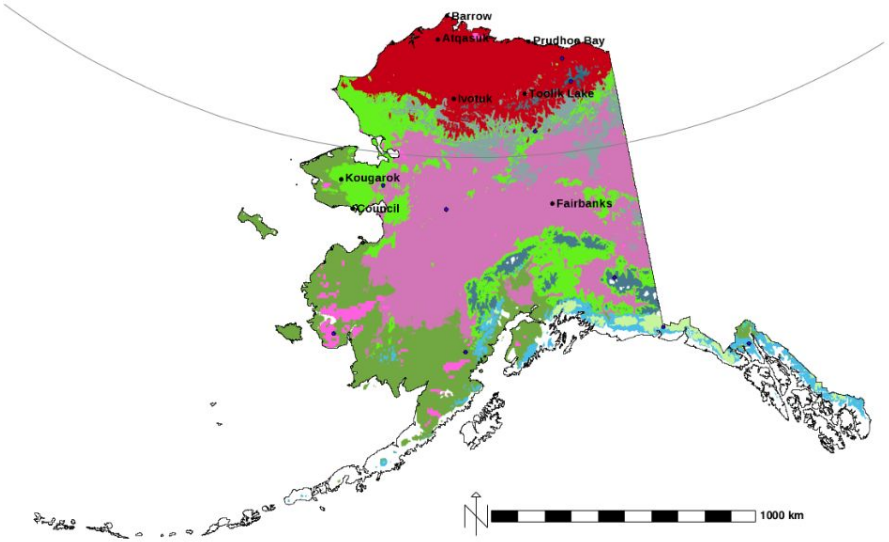

2090–2099

- Since the random colors are the same in both maps, a change in color represents an environmental change between the present and the future.
- At this level of division, the conditions in the large boreal forest become compressed onto the Brooks Range and the conditions on the Seward Peninsula “migrate” to the North Slope.

20 Alaska Ecoregions, Present and Future

(Hoffman et al., 2013)

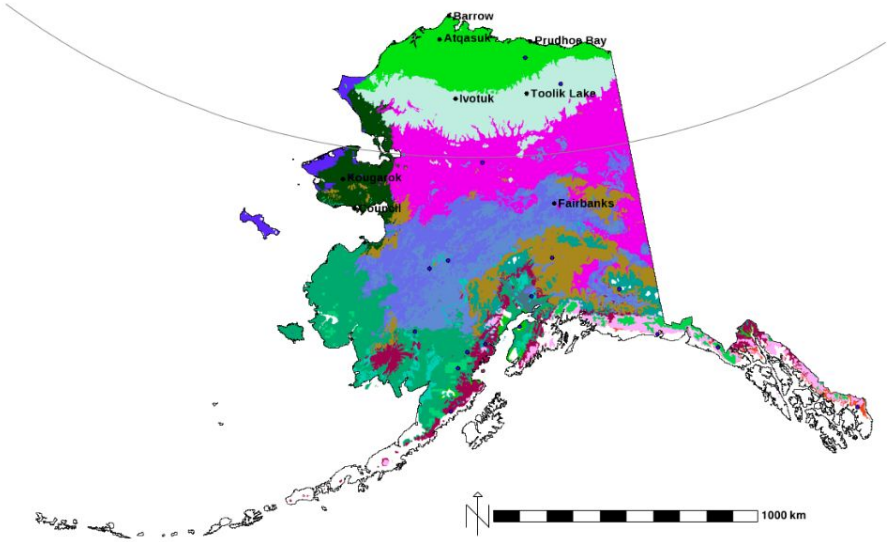

2000–2009

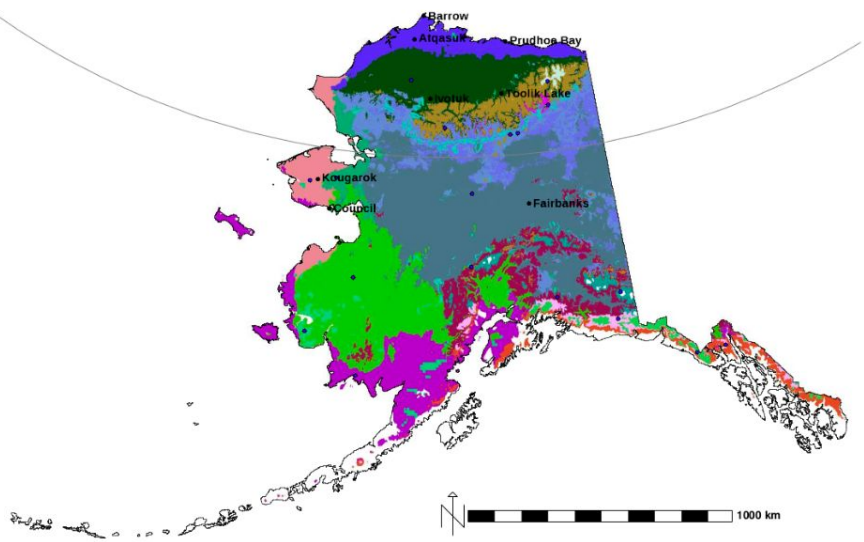

2090–2099

- Since the random colors are the same in both maps, a change in color represents an environmental change between the present and the future.
- At this level of division, the two primary regions of the Seward Peninsula and that of the northern boreal forest replace the two regions on the North Slope almost entirely.

Sampling Site Representativeness

- This representativeness analysis uses the standardized *n*-dimensional data space formed from all input data layers
- In this data space, the Euclidean distance between a sampling location (like Barrow) and every other point is calculated
- These data space distances are then used to generate grayscale maps showing the similarity, or lack thereof, of every location to the sampling location
- In the subsequent maps, white areas are well represented by the sampling location or network, while dark and black areas as poorly represented by the sampling location or network
- This analysis assumes that the climate surrogates maintain their predictive power and that no significant biological adaptation occurs in the future

Network Representativeness: Barrow vs. Barrow + Council

(Hoffman et al., 2013)

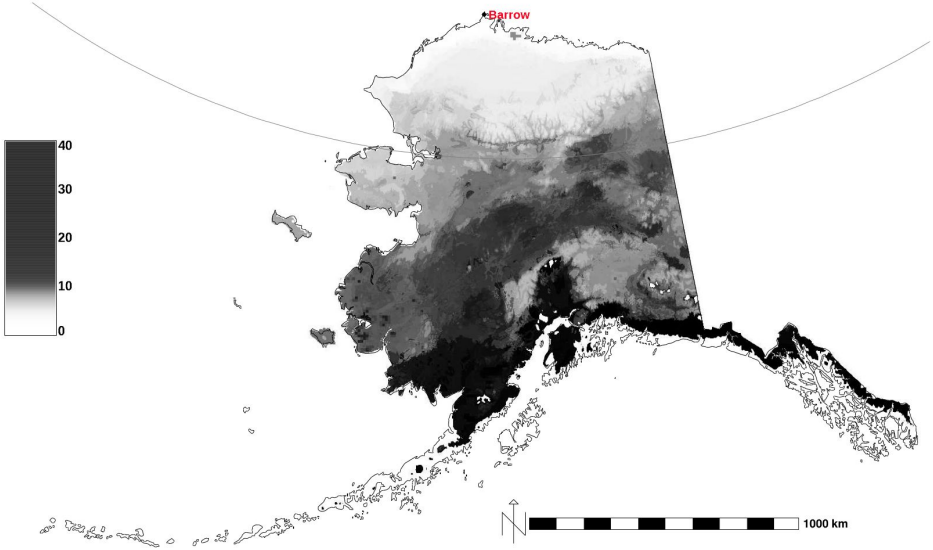

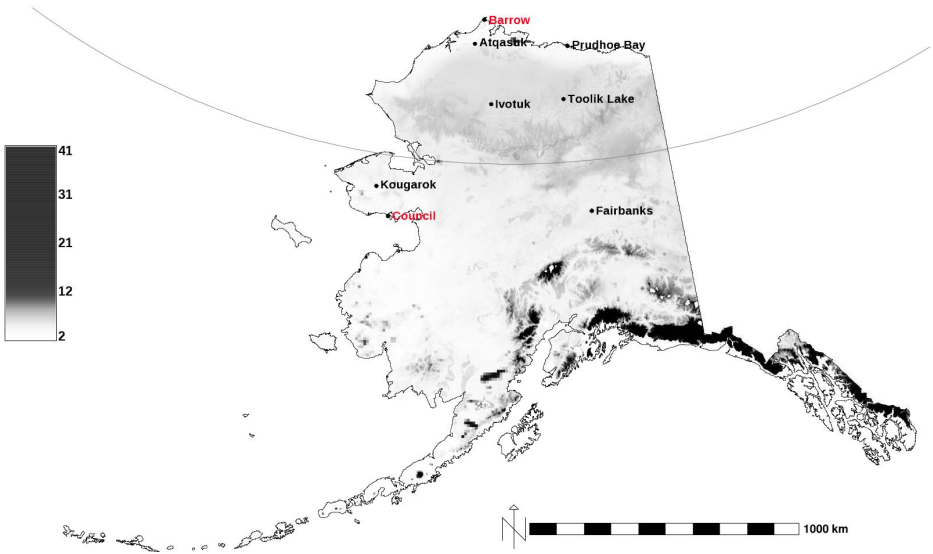

Light-colored regions are well represented and dark-colored regions are poorly represented by the sampling location listed in **red**.

State Space Dissimilarities: 8 Sites, Present (2000–2009)

Table: Site state space dissimilarities for the present (2000–2009).

Sites	Council	Atqasuk	Ivotuk	Toolik Lake	Kougarok	Prudhoe Bay	Fairbanks
Barrow	9.13	4.53	5.90	5.87	7.98	3.57	12.16
Council		8.69	6.37	7.00	2.28	8.15	5.05
Atqasuk			5.18	5.23	7.79	1.74	10.66
Ivotuk				1.81	5.83	4.48	7.90
Toolik Lake					6.47	4.65	8.70
Kougarok						7.25	5.57
Prudhoe Bay							10.38

State Space Dissimilarities: 8 Sites, Present and Future

Table: Site state space dissimilarities between the present (2000–2009) and the future (2090–2099).

		Future (2090–2099)							
	Sites	Barrow	Council	Atqasuk	Ivotuk	Toolik Lake	Kougarok	Prudhoe Bay	Fairbanks
Present (2000–2009)	Barrow	3.31	9.67	4.63	6.05	5.75	9.02	3.69	11.67
	Council	8.38	1.65	8.10	5.91	6.87	3.10	7.45	5.38
	Atqasuk	6.01	9.33	2.42	5.46	5.26	8.97	2.63	10.13
	Ivotuk	7.06	7.17	5.83	1.53	2.05	7.25	4.87	7.40
	Toolik Lake	7.19	7.67	6.07	2.48	1.25	7.70	5.23	8.16
	Kougarok	7.29	3.05	6.92	5.57	6.31	2.51	6.54	5.75
	Prudhoe Bay	5.29	8.80	3.07	4.75	4.69	8.48	1.94	9.81
	Fairbanks	12.02	5.49	10.36	7.83	8.74	6.24	10.10	1.96

Sampling Network Design

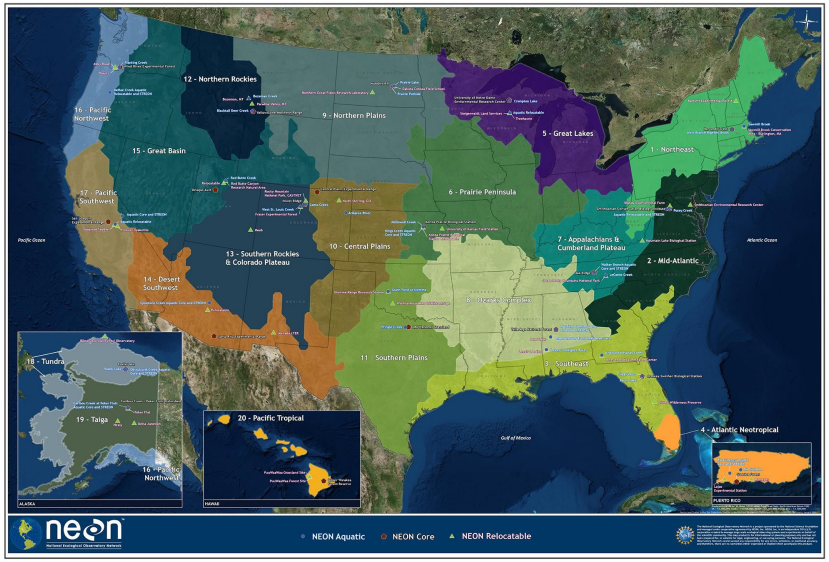

NSF's NEON Sampling Domains

Gridded data from satellite and airborne remote sensing, models, and synthesis products can be combined to design optimal sampling networks and understand representativeness as it evolves through time

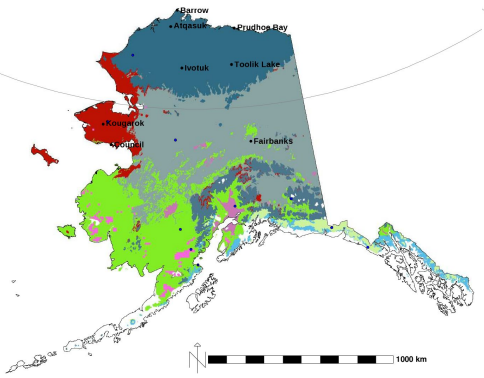

2000–2009

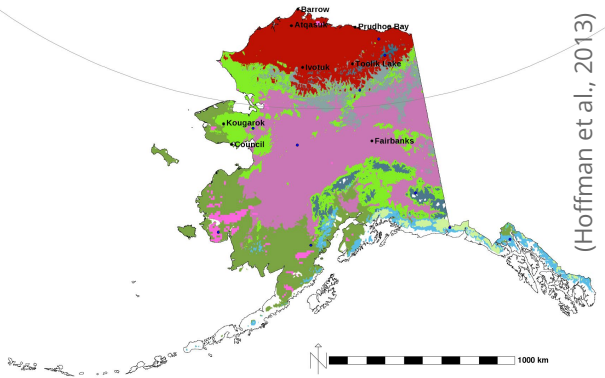

2090–2000

(Hoffman et al., 2013)

Triple-Network Global Representativeness

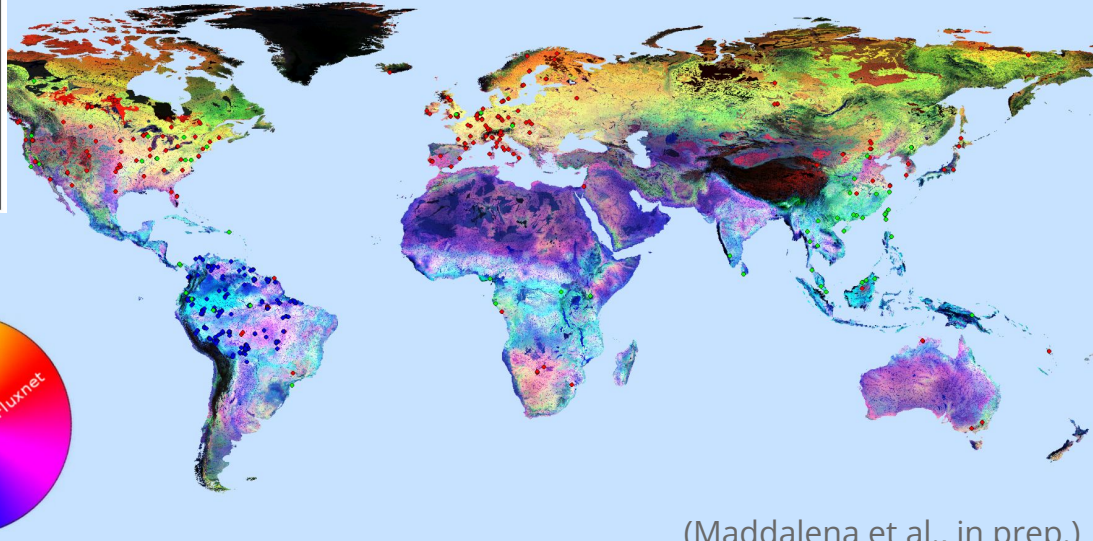

(Maddalena et al., in prep.)

50 Phenoregions for year 2012 (Random Colors)

250m MODIS NDVI
Every 8 days (46 images/year)
Clustered from year 2000 to present

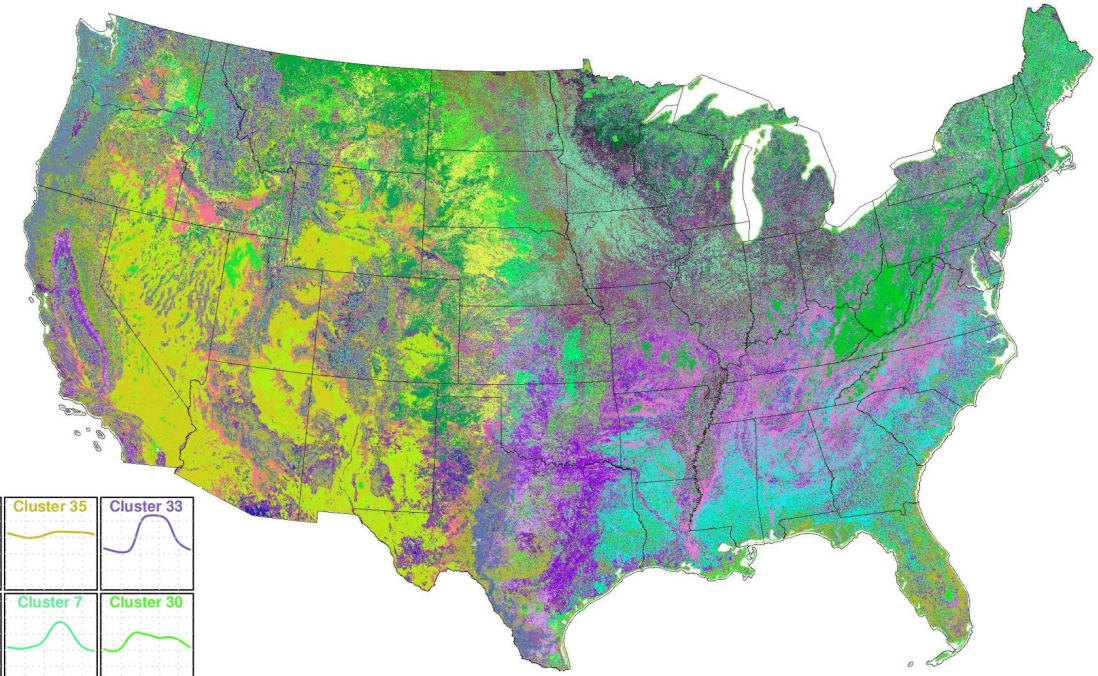

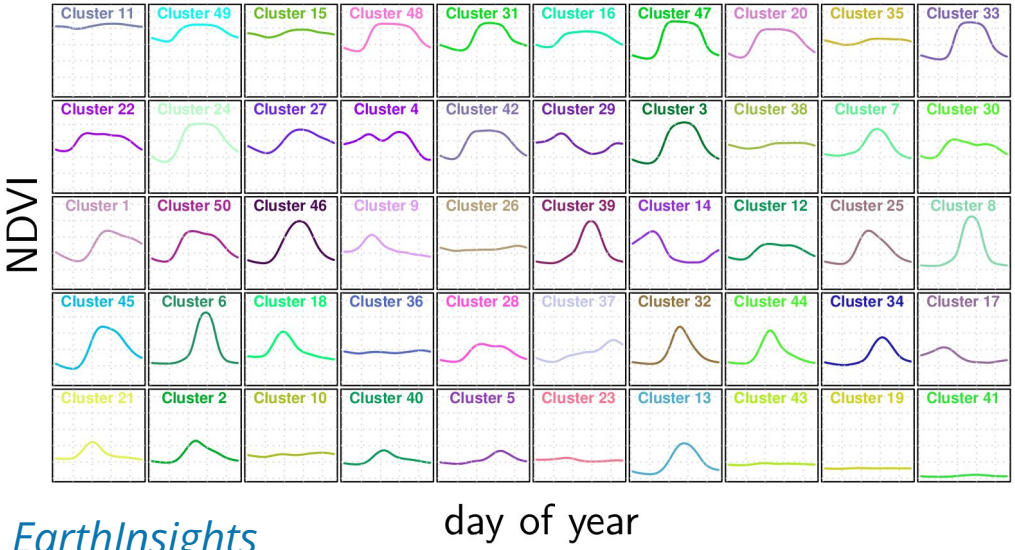

50 Phenoregion Prototypes (Random Colors)

EarthInsights

(Hargrove et al., in prep.)

50 Phenoregions Persistence and 50 Phenoregions Max Mode (Similarity Colors)

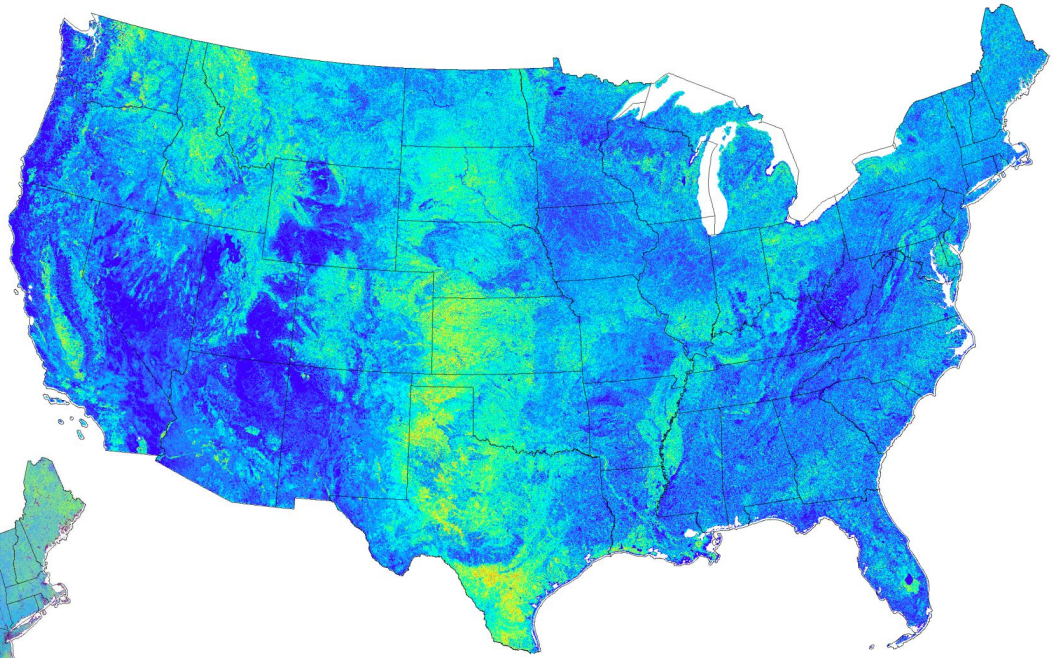

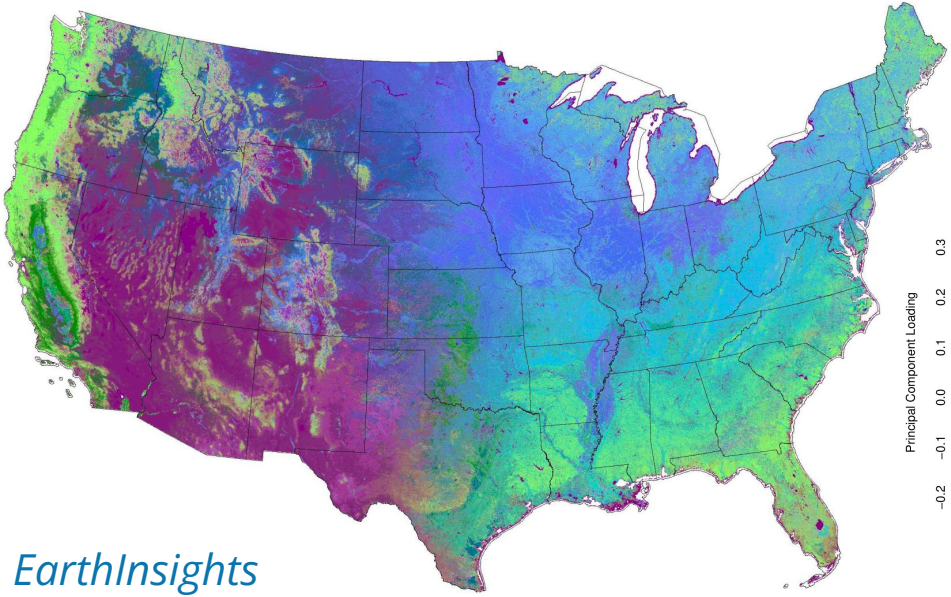

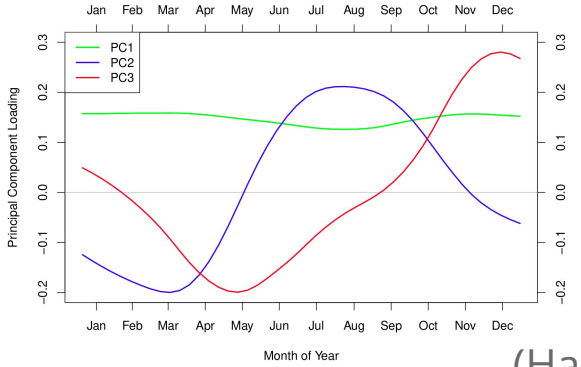

Principal Components Analysis

PC1 ~ Evergreen
PC2 ~ Deciduous
PC3 ~ Dry Deciduous

EarthInsights

(Hargrove et al., in prep.)

GSMNP: Spatial distribution of the 30 vegetation clusters across the national park

Extracted canopy height and structure from airborne LiDAR

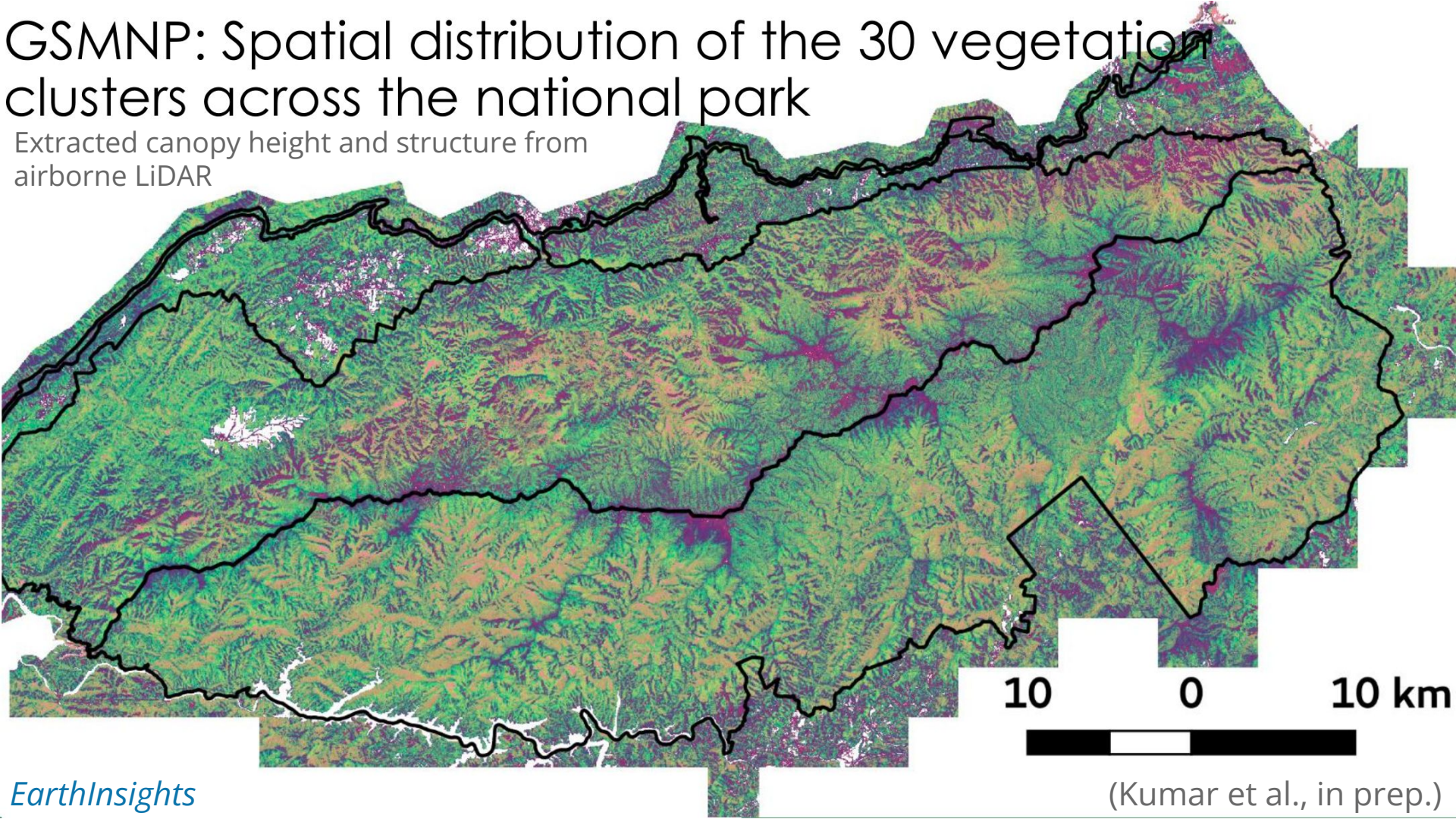

EarthInsights

(Kumar et al., in prep.)

GSMNP: 30 representative vertical structures (cluster centroids) identified

tall forests with low understory vegetation

forests with slightly lower mean height with dense understory vegetation

low height grasslands and heath balds that are small in area but distinct landscape type

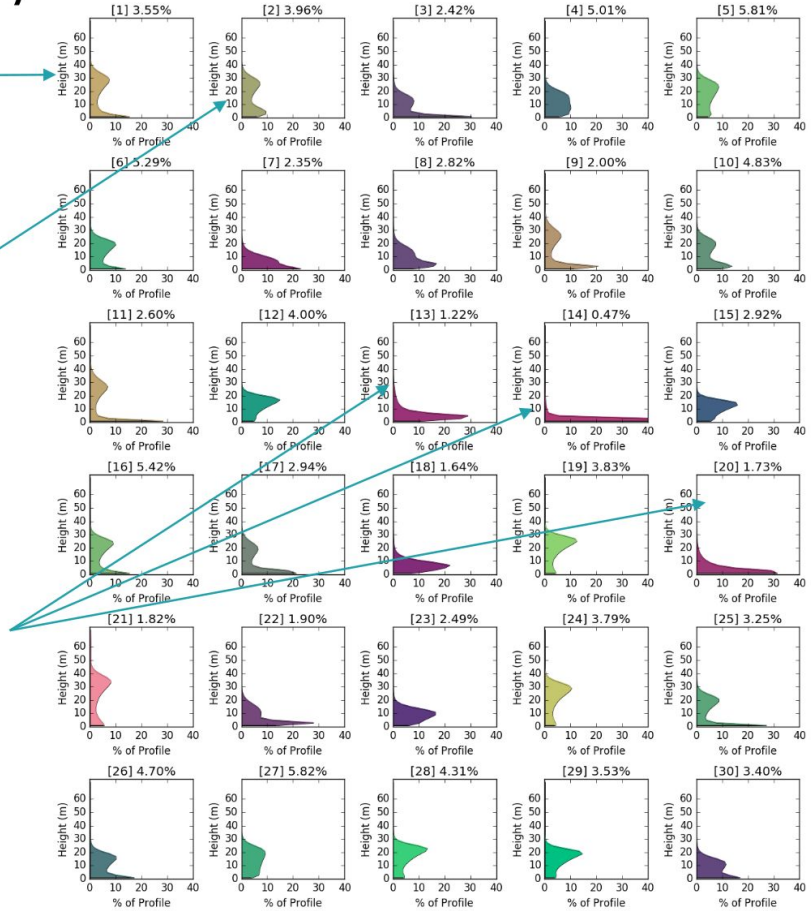

(Kumar et al., in prep.)

Global Fire Regimes

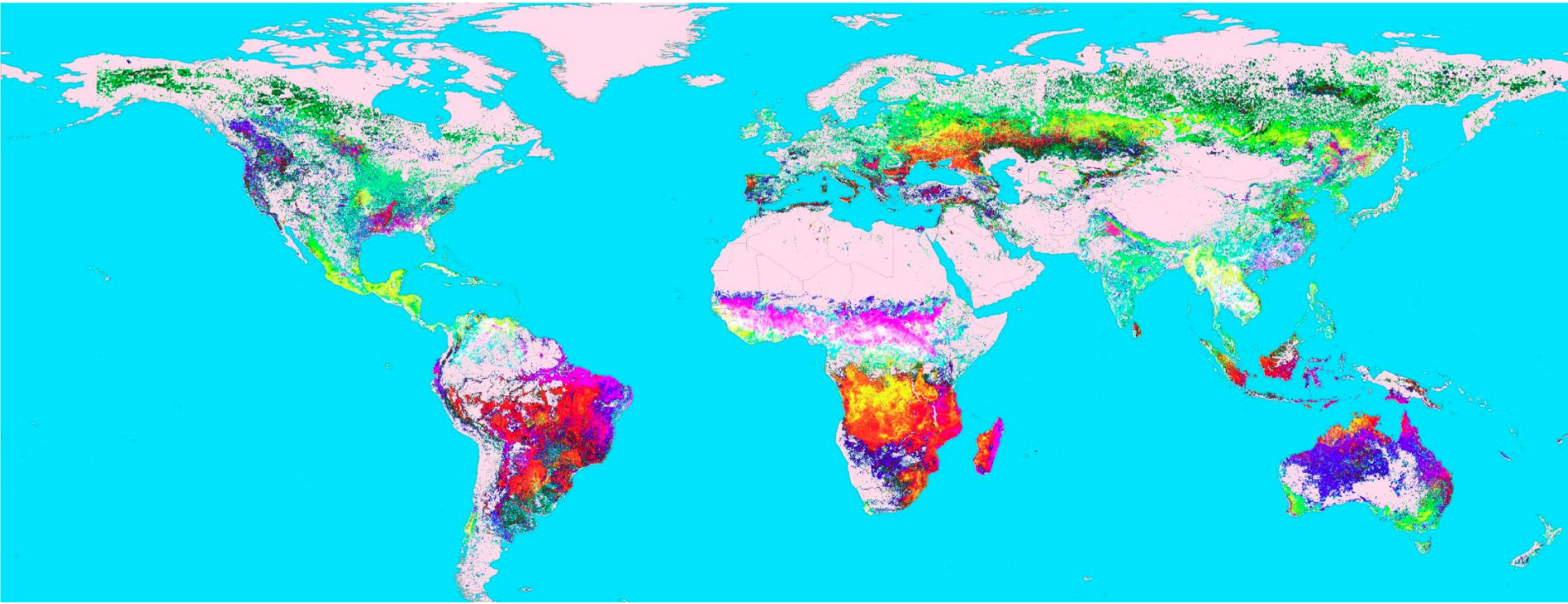

Regions that exhibit similar fire seasonality globally

From MODIS “Hotspots” at 1 km resolution from 2002–2018

EarthInsights

(Norman et al., submitted)

Vegetation Distribution at Barrow Environmental Observatory

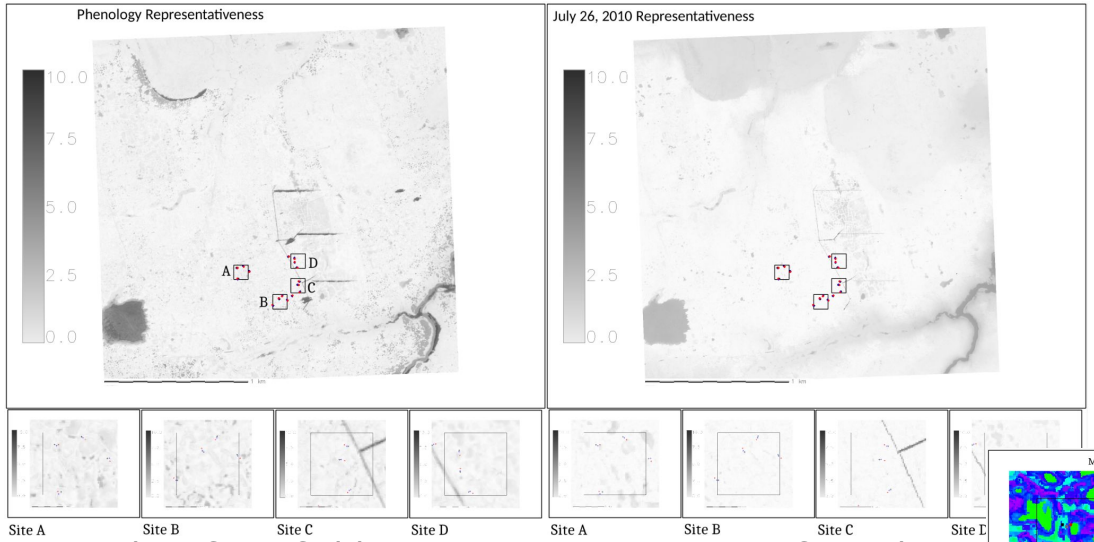

Representativeness map for vegetation sampling points in sites A, B, C, and D with phenology (left) and without (right) from WorldView2 multispectral imagery for the year 2010 and LiDAR data

Example plant functional type (PFT) distributions scaled up from vegetation sampling locations

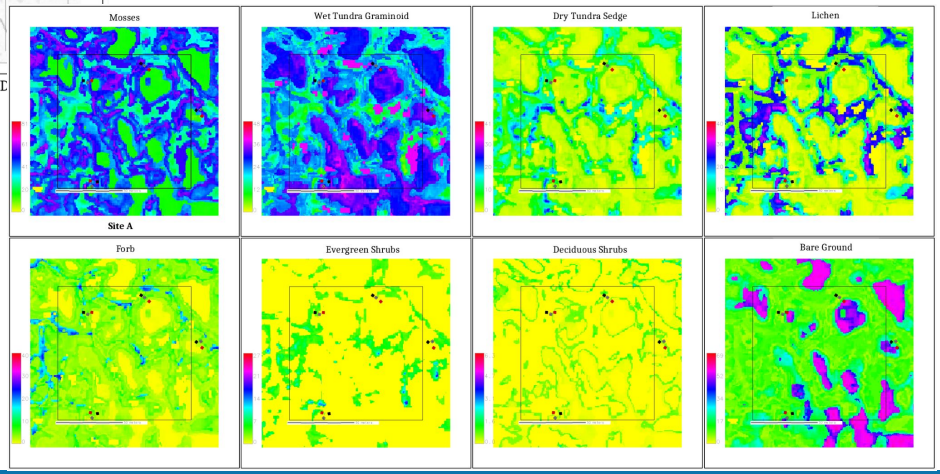

In situ data from field measurement activities inform the development of wide-scale maps of vegetation distribution through inference using remote sensing data as surrogate variables, and relationships with environmental controls can be extracted

Langford, Z. L., et al. (2016), Mapping Arctic Plant Functional Type Distributions in the Barrow Environmental Observatory Using WorldView-2 and LiDAR Datasets, *Remote Sens.*, 8(9):733, doi:10.3390/rs8090733.

Arctic Vegetation Mapping from Multi-Sensor Fusion

Used Hyperion Multispectral and IfSAR-derived Digital Elevation Model, applied cluster analysis, and trained a convolutional neural network (CNN) with Alaska Existing Vegetation Ecoregions (AKEVT)

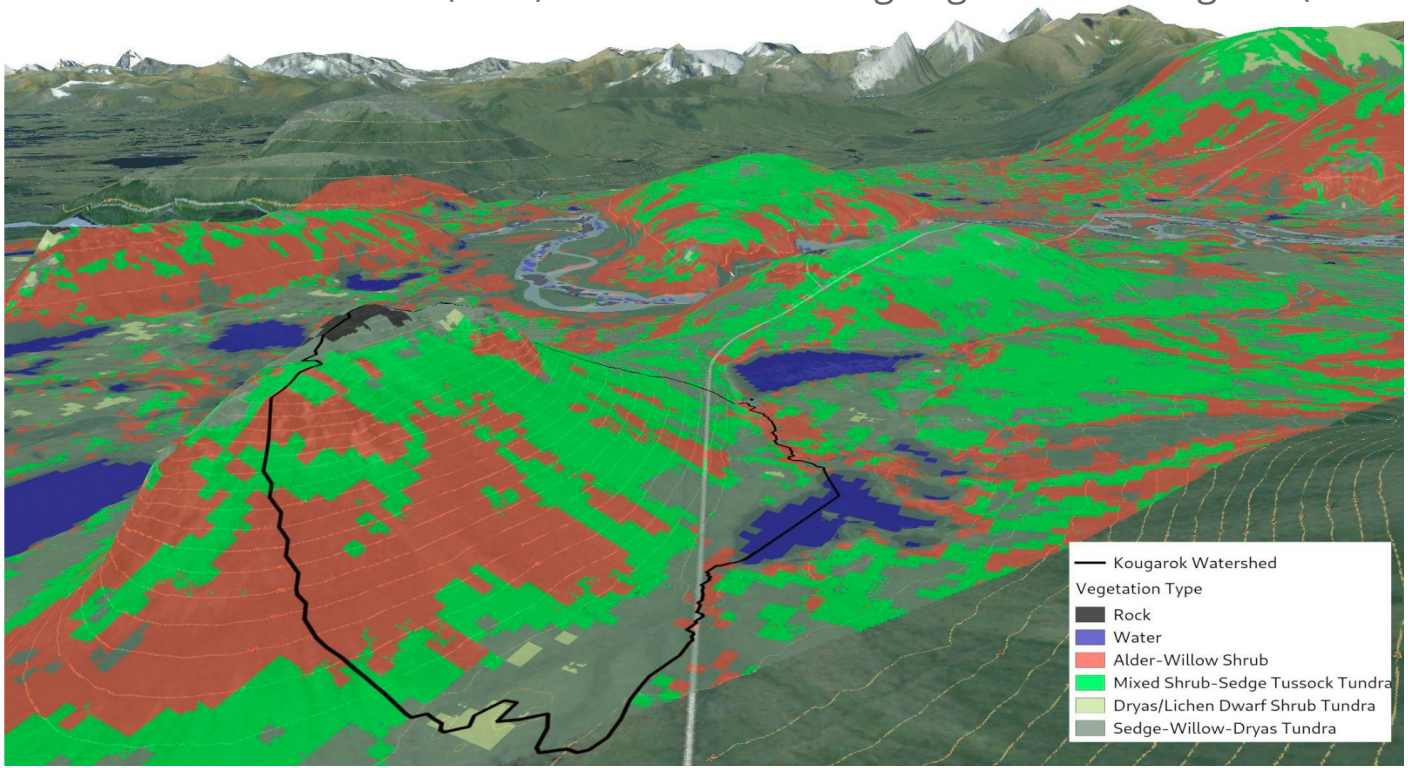

Langford, Z. L., et al. (2019), Arctic Vegetation Mapping Using Unsupervised Training Datasets and Convolutional Neural Networks, *Remote Sens.*, 11(1):69, doi:10.3390/rs11010069.

Satellite Data Analytics Enables Within-Season Crop Identification

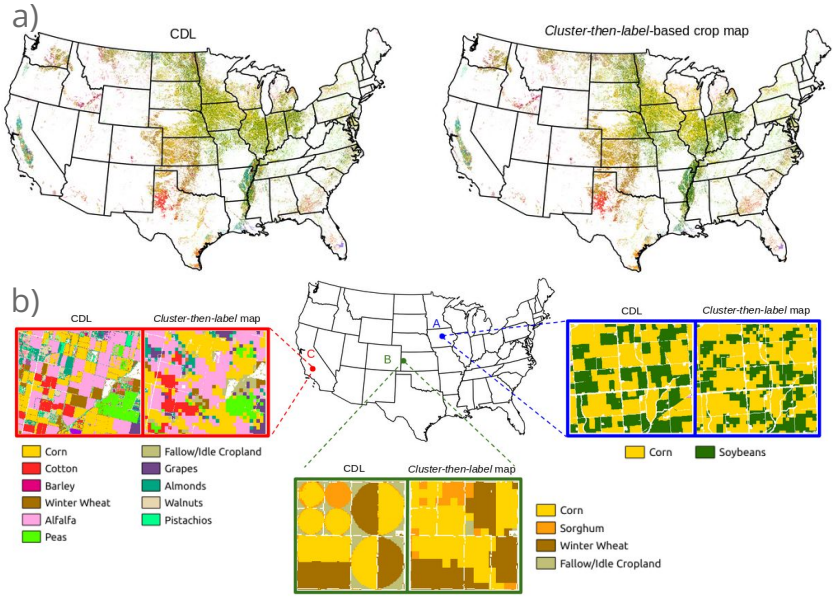

Figure: a) Comparison of cluster-then-label crop map with USDA Crop Data Layer (CDL) shows similar patterns at continental scale. b) Good spatial agreement is found at three selected regions, but cluster-then-label crop maps lack sharpness at field boundaries due to coarser resolution of MODIS data.

Earliest date for crop type classification

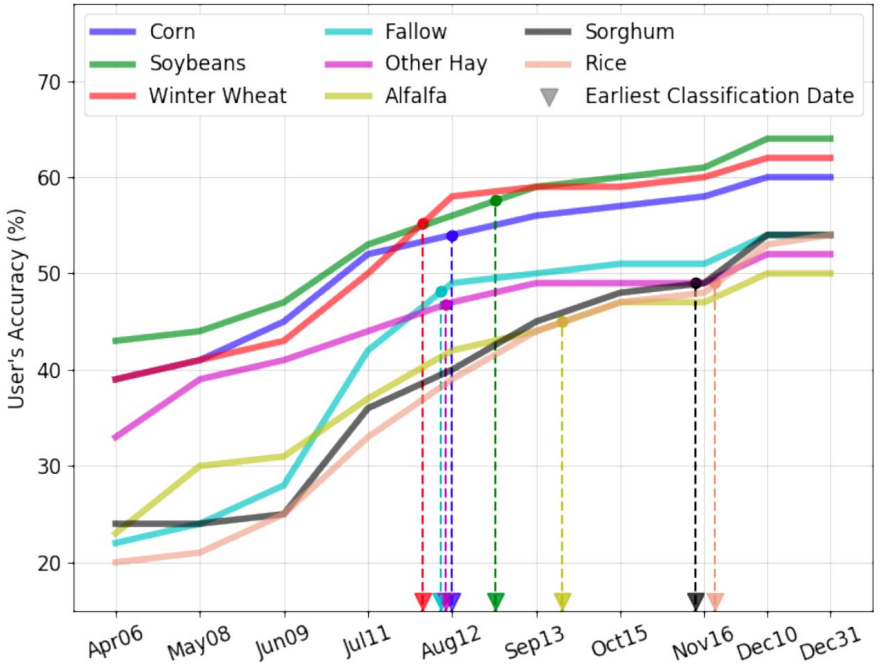

Konduri, V. S., J. Kumar, W. W. Hargrove, F. M. Hoffman, and A. R. Ganguly (2020), Mapping Crops Within the Growing Season Across the United States, *Remote Sens. Environ.*, 251, 112048, doi:10.1016/j.rse.2020.112048.

Watershed-Scale Plant Communities Determined from DNN and AVIRIS-NG

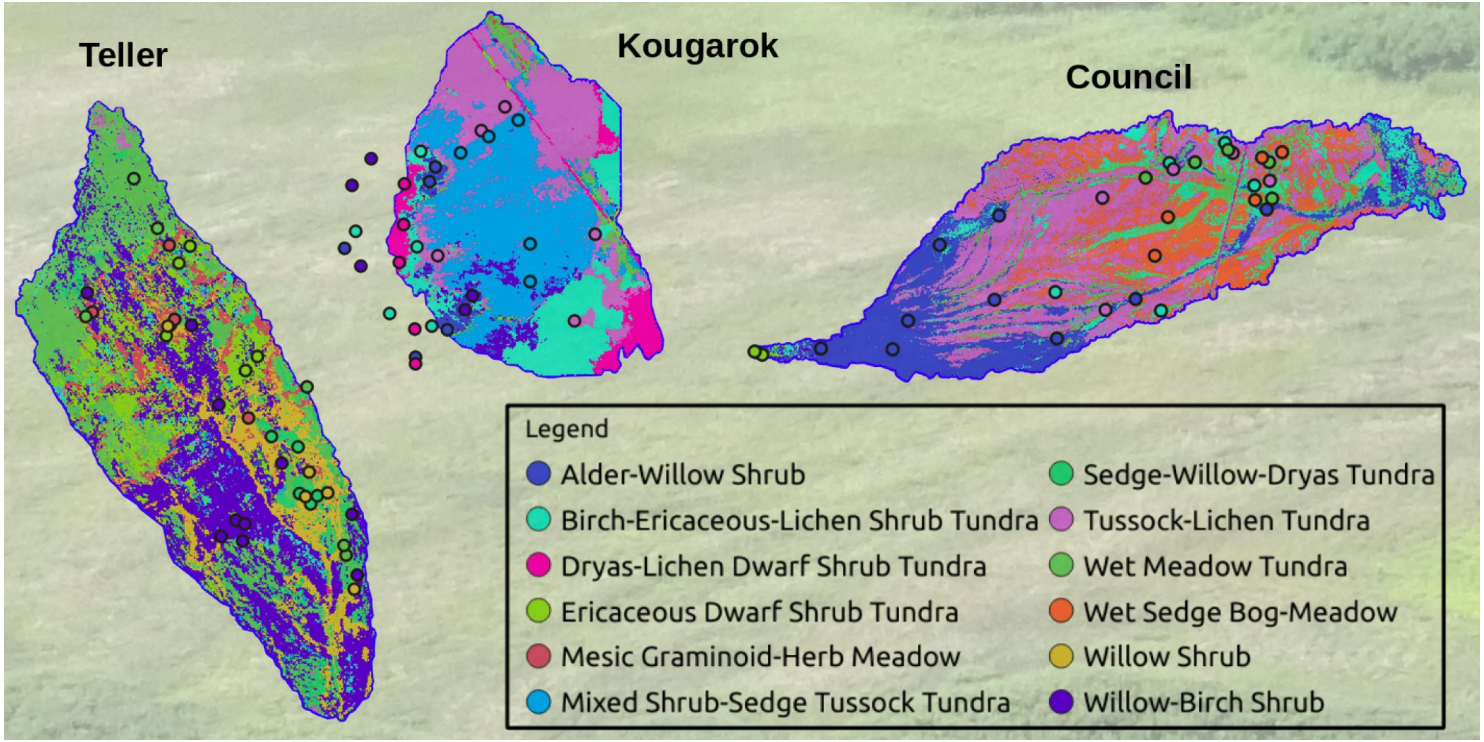

At the watershed scale, vegetation community distribution follows topographic and water controls. At a fine scale, nutrients limit the distribution of vegetation types.

(Konduri et al., in prep.)

Climate Change Mitigation through Climate Intervention

- The increasing severity of extreme events and wildfire is threatening utilities, built infrastructure, and economic & national security
- Loss of life and property is motivating consideration of *climate intervention* or *geoengineering*
- In addition to *carbon dioxide removal (CDR)* through *direct air capture (DAC)* and other means, interest is growing in reducing or stabilizing Earth's surface temperature
- *Solar radiation management (SRM)* is an approach to partially reduce warming, and *stratospheric aerosol intervention (SAI)* by injecting sulfur into the lower stratosphere is considered the most feasible scheme

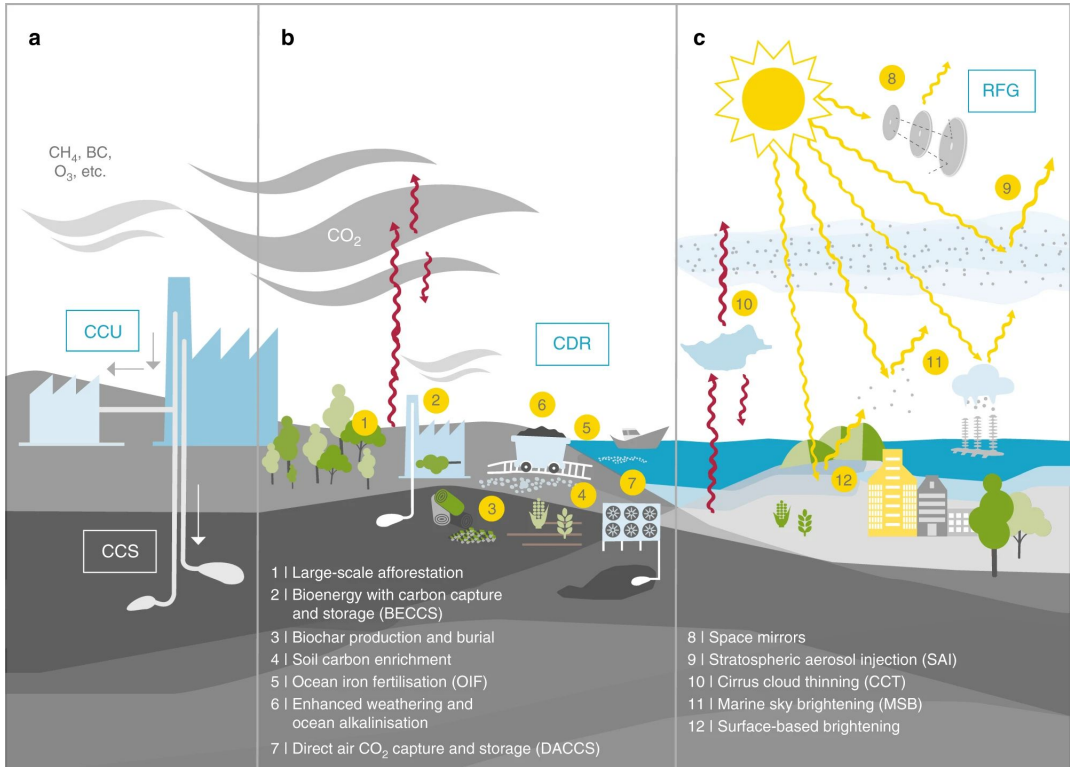

A wide variety of natural solutions and geoengineering techniques are proposed for mitigating the effects of climate change. Adopted from Lawrence et al. (2018).

Potential Ecological Impacts of Climate Intervention

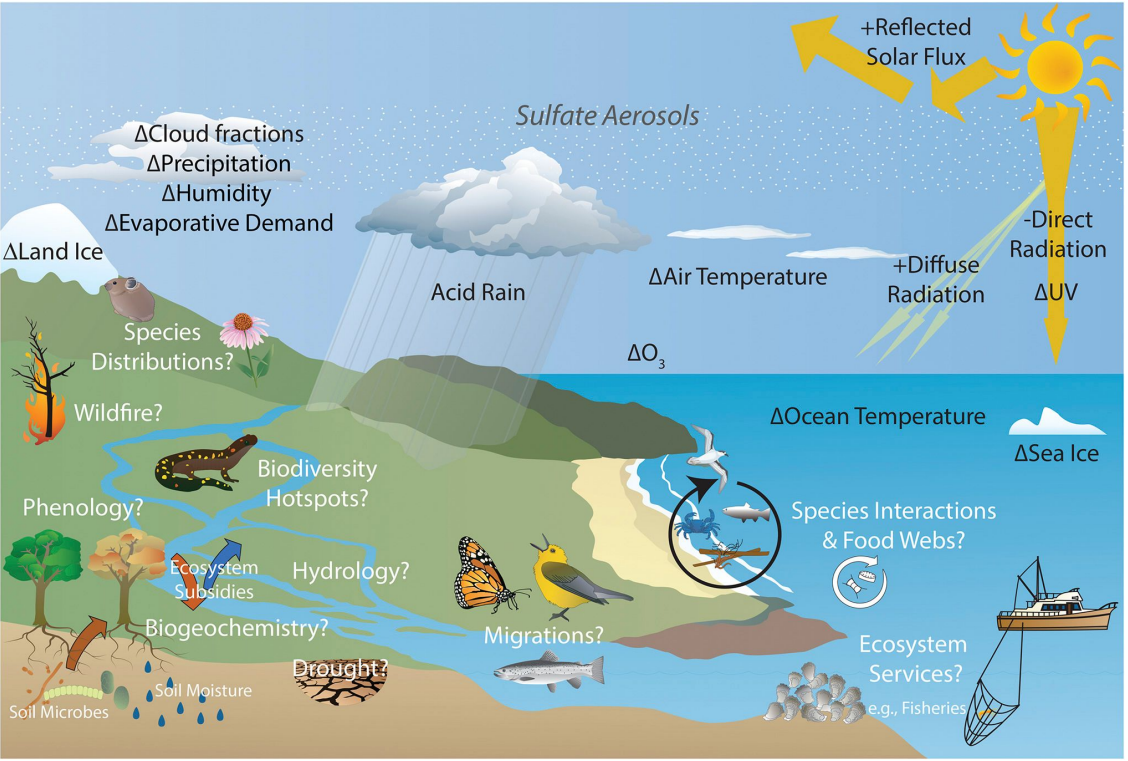

Although some effects of SRM with SAI on climate are known from certain SAI scenarios, the effects of SAI on ecological systems are largely unknown. Adopted from Zarnetske et al. (2021).

- While climate research has focused on predicted climate effects of SRM, few studies have investigated impacts that SRM would have on ecological systems
- Impacts and risks posed by SRM would vary by implementation scenario, anthropogenic climate effects, geographic region, and by ecosystem, community, population, and organism
- A transdisciplinary approach is essential, and **new modeling paradigms are required**, to represent complex interactions across Earth system components, scales, and ecological systems

Climate Intervention Research

A 2021 report from the National Academies of Sciences, Engineering, and Medicine (NASEM) concludes **a strategic investment in research is needed** to advance policymakers' understanding of climate response options.

> *The US should develop a transdisciplinary research program, in collaboration with other nations, to advance understanding of solar geoengineering's technical feasibility and effectiveness, possible impacts on society and the environment, and social dimensions such as public perceptions, political and economic dynamics, and ethical and equity considerations.*

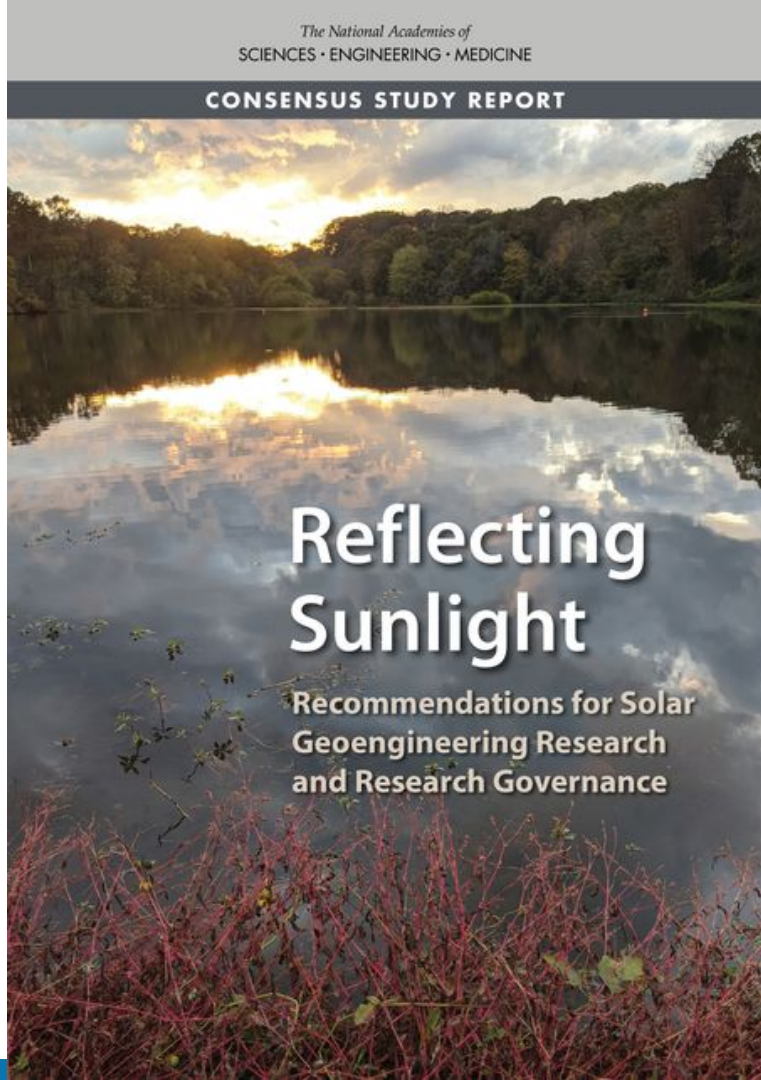

Geoengineering Increases the Global Land Carbon Sink

Objective: To examine stratospheric aerosol intervention (SAI) impacts on plant productivity and terrestrial biogeochemistry.

Approach: Analyze and compare simulation results from the Stratospheric Aerosol Geoengineering Large Ensemble (GLENS) project from 2010 to 2097 under RCP8.5 with and without SAI.

Results/Impacts: In this scenario, SAI causes terrestrial ecosystems to store an additional 79 Pg C globally as a result of lower ecosystem respiration and diminished disturbance effects by the end of the 21st century, yielding as much as a 4% reduction in atmospheric CO_2 mole fraction that progressively reduces the SAI effort required to stabilize surface temperature.

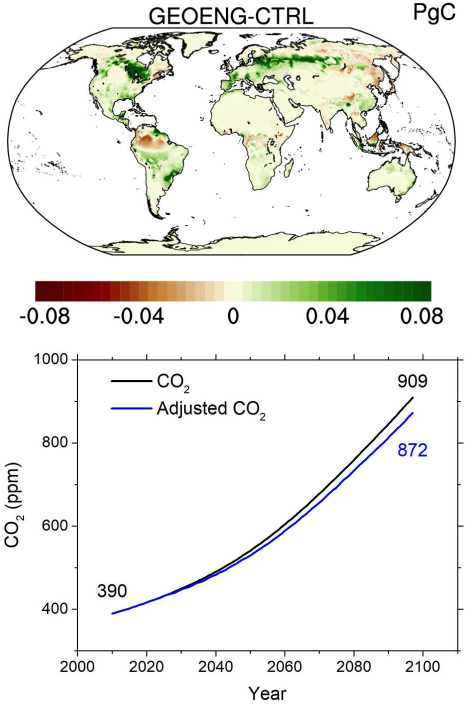

Figure: The larger sink under SAI increased land C storage by 79 Pg C by 2097, which would reduce the projected atmospheric CO_2 level.

Yang, C.-E., **F. M. Hoffman**, D. M. Ricciuto, S. Tilmes, L. Xia, D. G. MacMartin, B. Kravitz, J. H. Richter, M. Mills, and J. S. Fu (2020), Assessing Terrestrial Biogeochemical Feedbacks in a Strategically Geoengineered Climate, *Environ. Res. Lett.*, doi:10.1088/1748-9326/abacf7.

Exploring Feedbacks of SAI

- To fill research gaps in understanding Earth system feedbacks of SAI on ecosystems, we are conducting a series of increasingly complex geoengineering simulations with **DOE's Energy Exascale Earth System Model (E3SM)**
- **Simulations will mimic effects of CDR, SAI, and CDR plus SAI**
- Start with SSP5-3.4-OS mid-range overshoot CO_2 trajectory from CMIP6, which prescribes a drawdown of CO_2
- Global surface temperatures will rise by >2.5°C around 2040, **above the 2°C threshold that may induce irreversible impacts**
- Next, introduce SAI to simultaneously cool the surface until drawdown is sufficient to assure < 2°C warming, called **temperature "peak shaving"**
- To quantify feedbacks from reducing, not increasing, atmospheric CO_2, **but may not capture all the as yet unobserved processes**

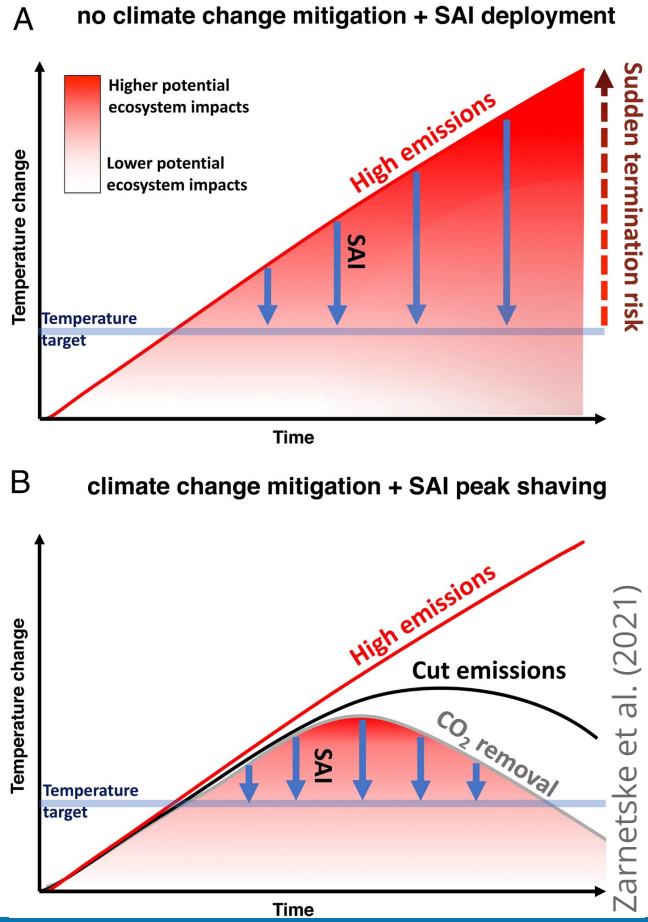

Leveraging Advances in Machine Learning for Earth Sciences

Existing machine learning techniques can improve understanding of biospheric processes and representation in Earth system models

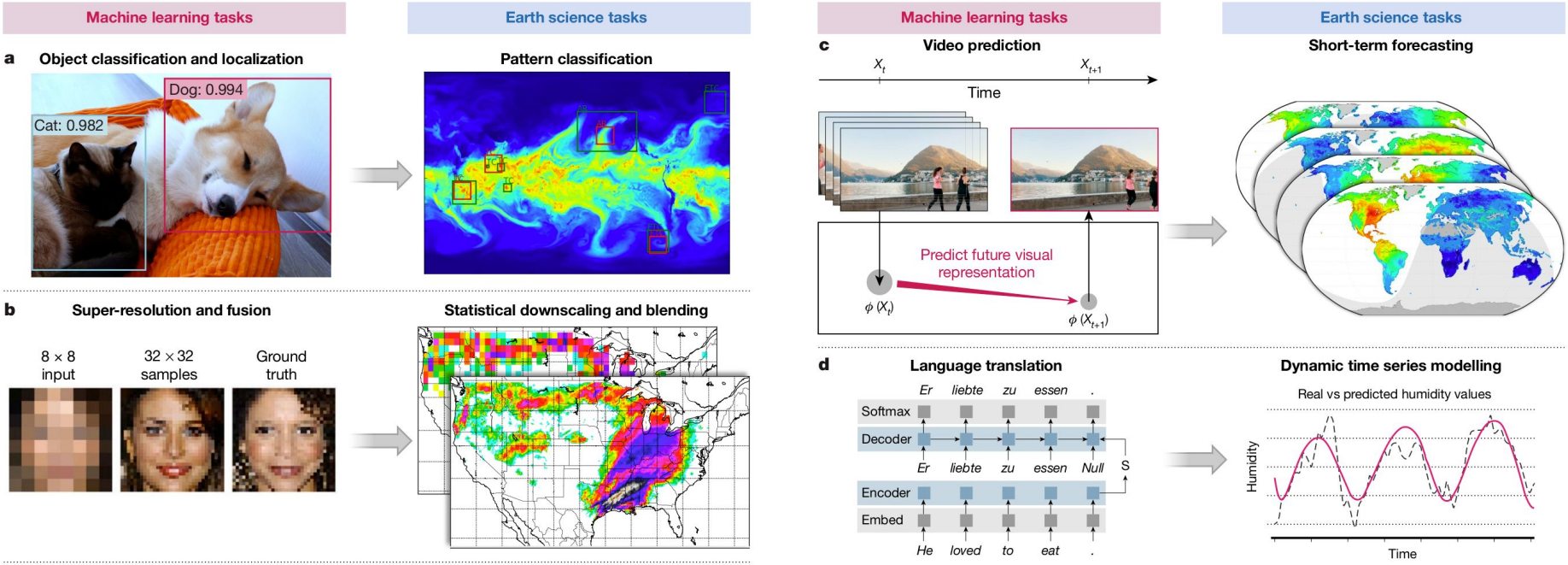

Figure 2 in Reichstein et al. (2019)

Machine Learning for Understanding Biospheric Processes

- Widening adoption of deep neural networks and growth of climate data are fueling interest in AI/ML for use in weather and climate and Earth system models
- ML potential is high for improving predictability when (1) *sufficient data are available for process representations* and (2) *process representations are computationally expensive*
- Example methods for improving ELM capabilities by exploring ML and information theory approaches:
  - **Soil organic carbon & radiocarbon**
  - **Wildfire**
  - **Methane emissions**
  - **Ecohydrology**
- All of these applications involve unresolved, subgrid-scale processes that strongly influence results at the largest scales

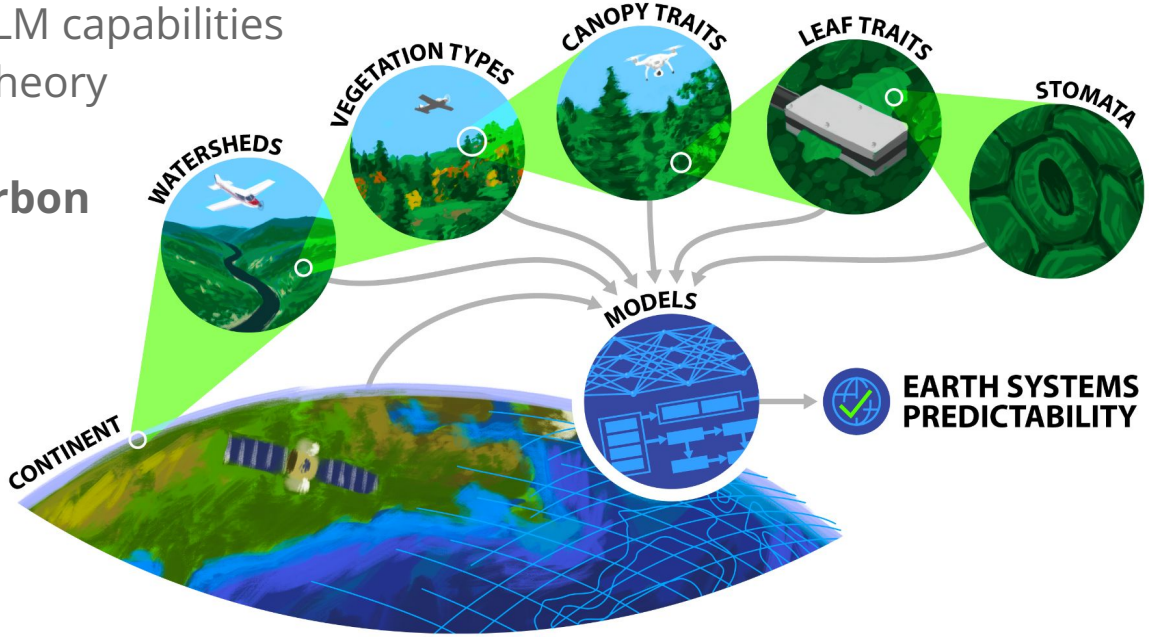

Hybrid Modeling of Wildfire Activities

- Improve model simulations of **wildfire processes**, including ignition, fire duration, and spread rate with Deep Neural Network models
- Improve simulated **wildfire emissions** and their impacts on atmospheric properties, including aerosols, greenhouse gases, phosphorus transport, and pollutants
- Improve the projection of near-future and long-term dynamics of wildfire activities
- Accelerate E3SM coupled land–atmosphere modeling activities for wildfire research
- Explore online ML training/validation strategy for E3SM coupled model simulations

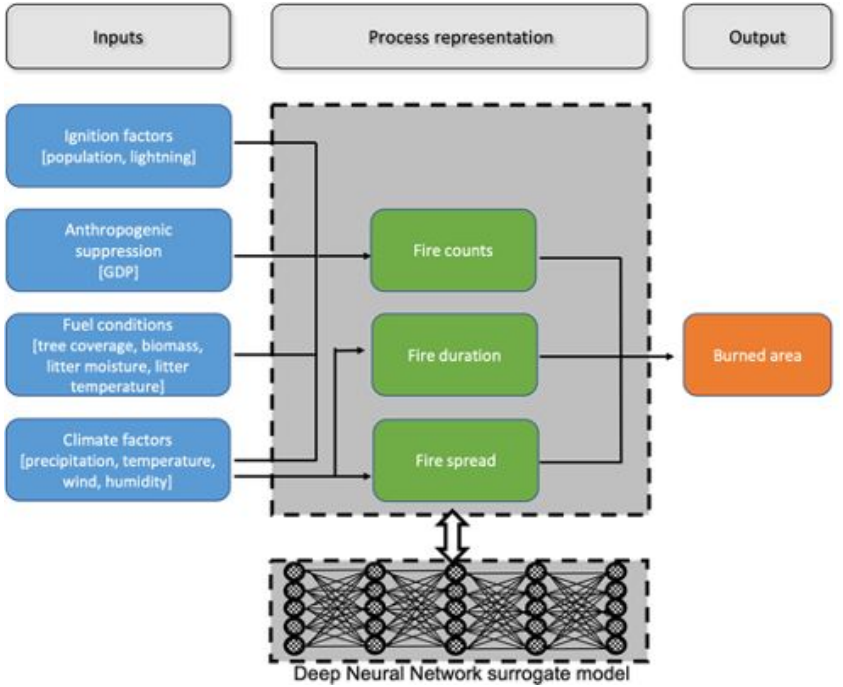

Zhu et al. (2022)

Hybrid ML/Process-based Modeling for Terrestrial Modeling

In the hierarchy of land model processes, we start with the **photosynthesis** parameterization because

- Multiple hypotheses
- Many leaf-level measurements
- Most computationally intensive part of the land model

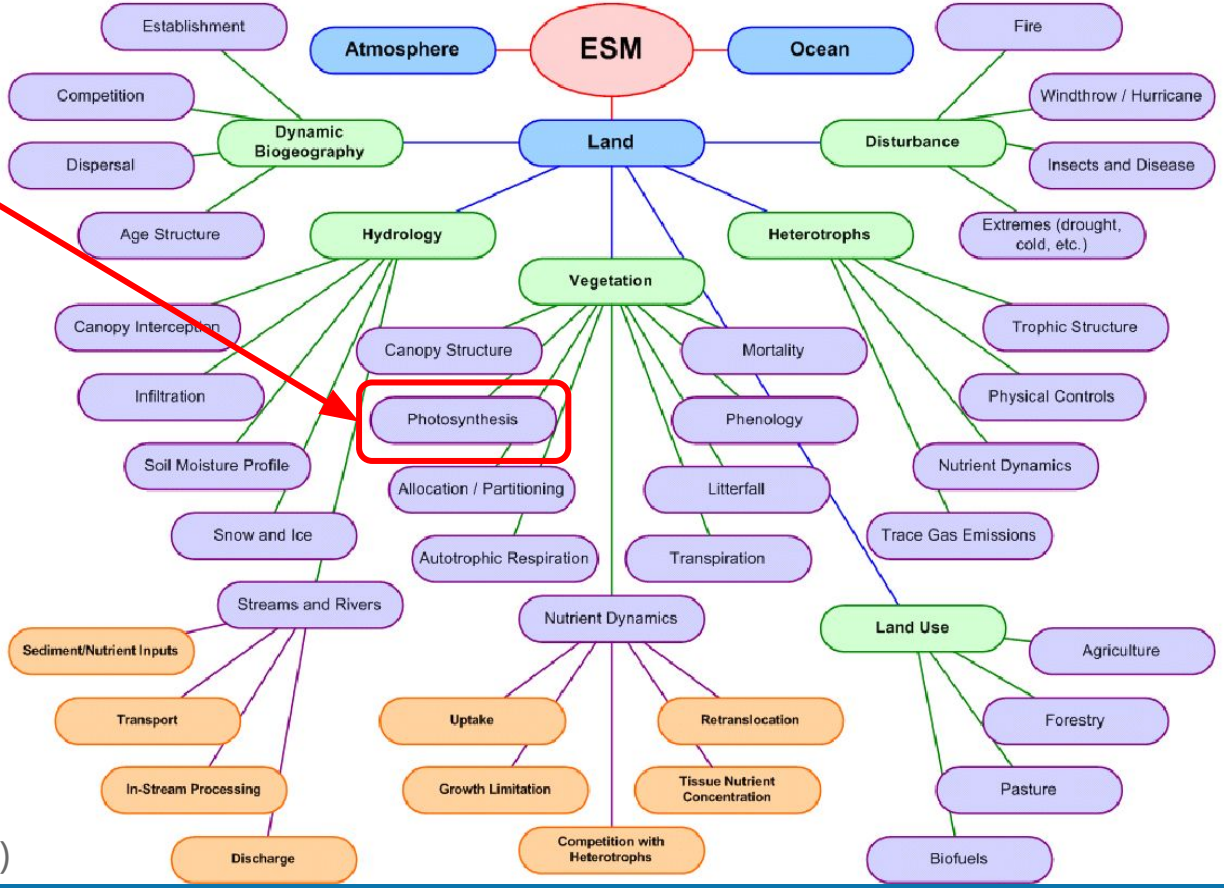

(Figure from P. E. Thornton)

Hybrid ML/Process-based Modeling for Terrestrial Modeling

Individual processes can be represented by a multi-hypothesis approach, and ML provides an opportunity for a data-derived hypothesis that can be further explored or used to calibrate other hypotheses, when sufficient data are available.

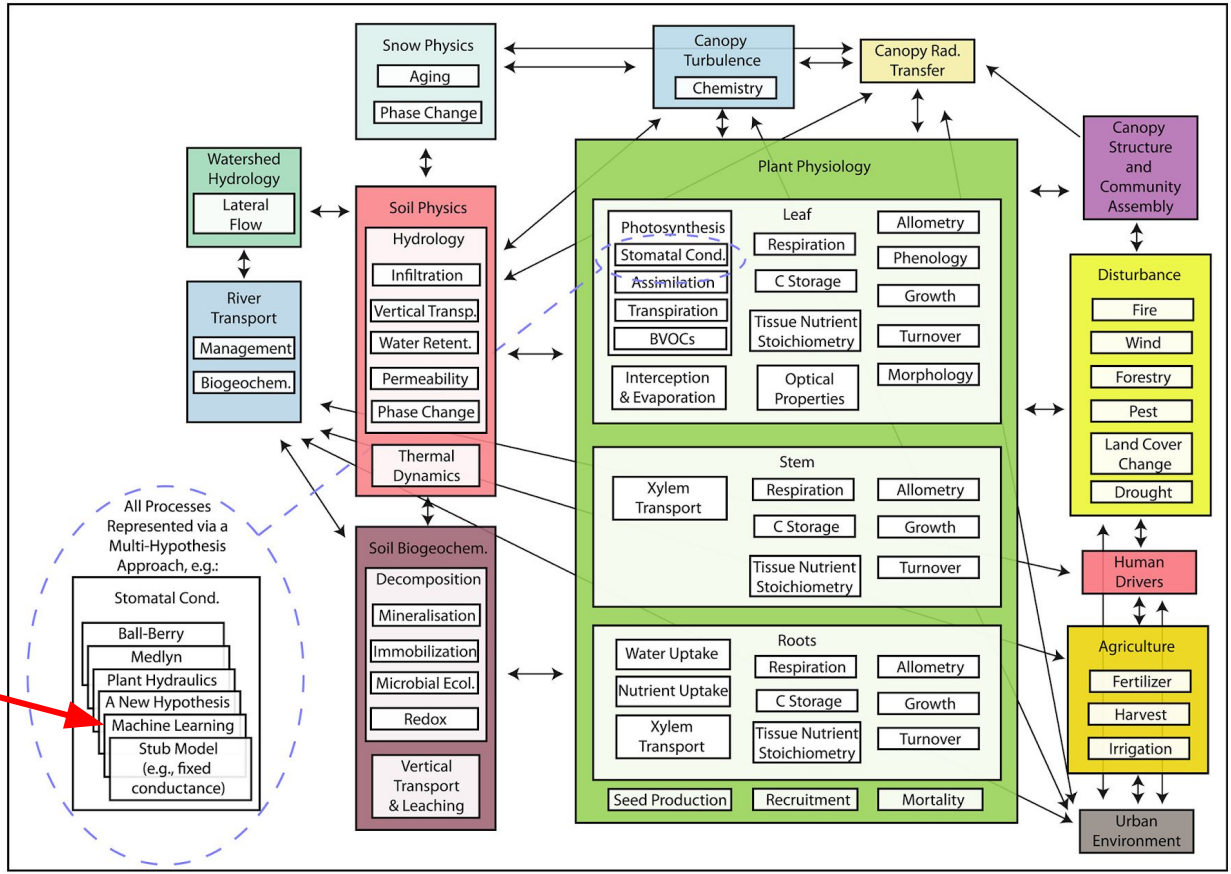

(a) Process Schematic of a Possible Full-Complexity Configuration of a Land Surface Model

(Fisher and Koven, 2020)

AI-Constrained Ecohydrology for Improving Earth System Predictions

Collaboration among ORNL, LANL, Penn State, et al.

Contact: Forrest M. Hoffman

Project to prototype machine learning-based parameterizations for stomatal conductance and photosynthesis

- Photosynthesis is a computationally expensive part of land models and leaf-level flux and phenology data are available
- Use combinations of leaf-level and plant hydrodynamics data to build ML models of C_3, C_4, and CAM vegetation
- Investigate ML approaches for scaling to canopies and watersheds
- Prototype hybrid ML-/process-based components within the E3SM Land Model (ELM)
- Future efforts:
  - Conduct regional and global simulations to benchmark different combinations of process-based and ML modules
  - Explore approaches for building hybrid modeling interfaces within ELM

Nature

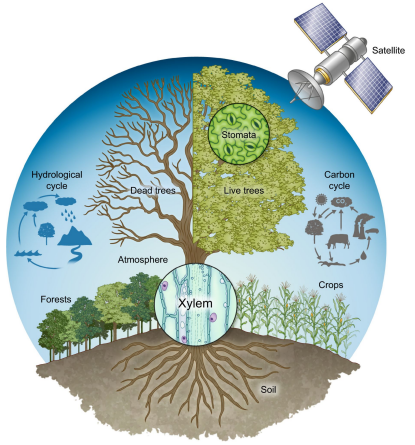

McDowell et al. (2019)

The Future is Bright for AI/ML in Earth System Science

A Convergence of New Technology, Explosive Data Growth, and Free Tools

- High performance computing (exascale in big centers and commercial cloud)
- Large data storage resources (commercial and on-premise cloud)
- High speed networks (e.g., ESnet) and data movement technologies (Globus)
- Satellites (shoebox CubeSats) and airborne (drones) platforms
- Cheap (free!) and easy-to-use ML tools (PyTorch, Keras, Scikit-Learn)

Future Applications Could Revolutionize Our Understanding and Ability to Predict

- Poorly understood processes and mechanisms can be mimicked with adequate amounts of data and advanced ML techniques
- Explainable AI and systematic approaches to modeling could lead to new scientific discoveries and improved understanding of the Earth system
- Predictions of complex, nonlinear, large-scale phenomena and natural hazards could be predicted with increasing accuracy

International Land Model Benchmarking (ILAMB)

What is a Benchmark?

- A **benchmark** is a quantitative test of model function achieved through comparison of model results with observational data
- Acceptable performance on a benchmark **is a necessary but not sufficient condition** for a fully functioning model
- **Functional relationship benchmarks** offer tests of model responses to forcings and yield insights into ecosystem processes
- Effective benchmarks must draw upon **a broad set of independent observations** to evaluate model performance at multiple scales

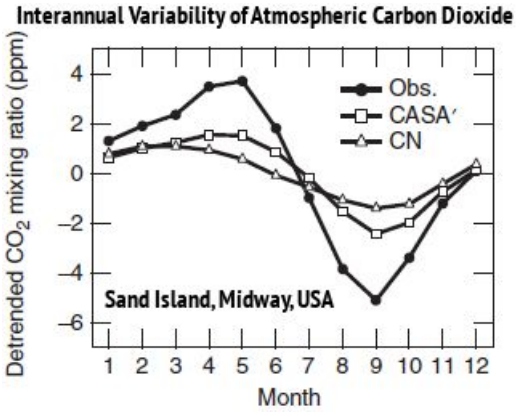

Models often fail to capture the amplitude of the seasonal cycle of atmospheric CO_2

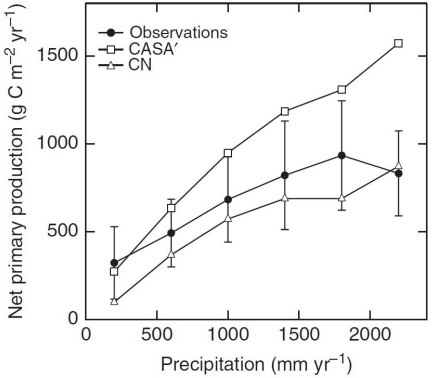

(Randerson et al., 2009)

Models may reproduce correct responses over only a limited range of forcing variables

Why Benchmark Models?

- To **quantify and reduce uncertainties** in carbon cycle feedbacks to improve projections of future climate change (Eyring et al., 2019; Collier et al., 2018)
- To **quantitatively diagnose impacts of model development** on hydrological and carbon cycle process representations and their interactions
- To **guide synthesis efforts**, such as the Intergovernmental Panel on Climate Change (IPCC), by determining which models are broadly consistent with available observations (Eyring et al., 2019)
- To **increase scrutiny of key datasets** used for model evaluation
- To **identify gaps in existing observations** needed to inform model development
- To **accelerate delivery of new measurement datasets** for rapid and widespread use in model assessment

What is ILAMB?

A community coordination activity created to:

- **Develop internationally accepted benchmarks** for land model performance by drawing upon collaborative expertise
- **Promote the use of these benchmarks** for model intercomparison
- **Strengthen linkages between experimental, remote sensing, and Earth system modeling communities** in the design of new model tests and new measurement programs
- **Support the design and development of open source benchmarking tools**

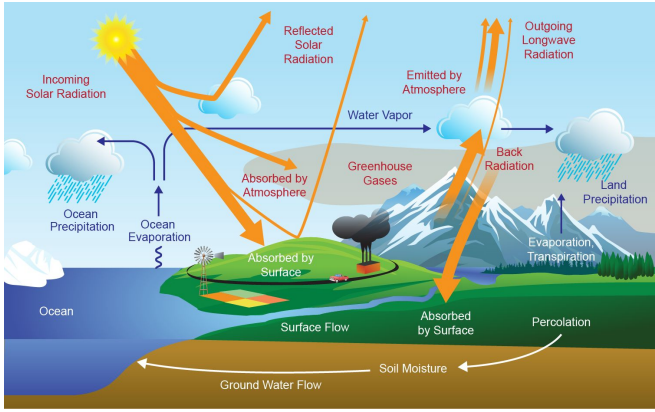

Energy and Water Cycles

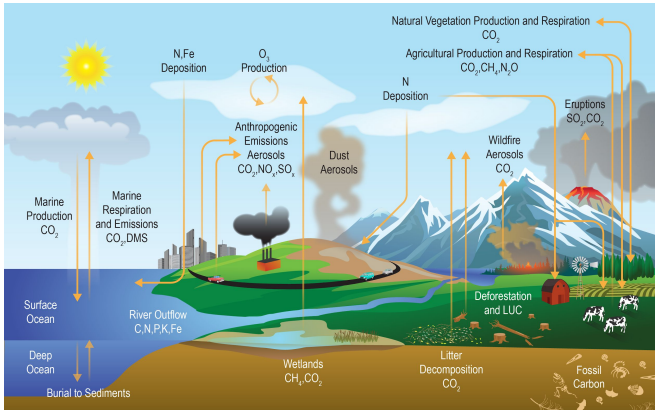

Carbon and Biogeochemical Cycles

2016 International Land Model Benchmarking (ILAMB) Workshop
May 16–18, 2016, Washington, DC

Third ILAMB Workshop was held May 16–18, 2016

- Workshop Goals
  - Design of new metrics for model benchmarking
  - Model Intercomparison Project (MIP) evaluation needs
  - Model development, testbeds, and workflow processes
  - Observational datasets and needed measurements
- Workshop Attendance
  - 60+ participants from Australia, Japan, China, Germany, Sweden, Netherlands, UK, and US (10 modeling centers)
  - ~25 remote attendees at any time

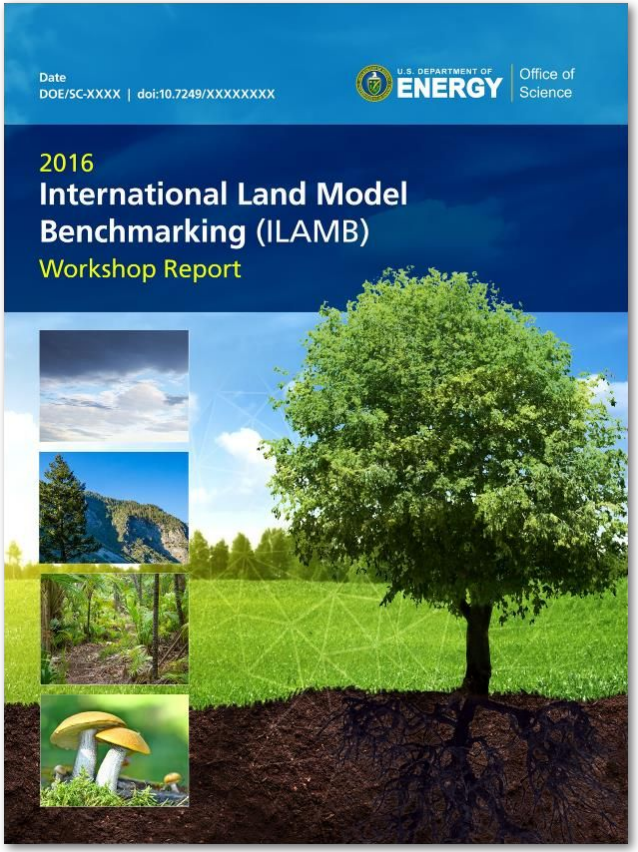

(Hoffman et al., 2017)

Argonne NATIONAL LABORATORY · BROOKHAVEN NATIONAL LABORATORY · BERKELEY LAB · Los Alamos NATIONAL LABORATORY · NCAR NATIONAL CENTER FOR ATMOSPHERIC RESEARCH · OAK RIDGE National Laboratory · UCI · MICHIGAN

Development of ILAMB Packages

- **ILAMBv1** released at 2015 AGU Fall Meeting Town Hall, doi:10.18139/ILAMB.v001.00/1251597
- **ILAMBv2** released at 2016 ILAMB Workshop, doi:10.18139/ILAMB.v002.00/1251621
- **Open Source software** written in Python; **runs in parallel** on laptops, clusters, and supercomputers
- Routinely used for land model evaluation during development of ESMs, including the **E3SM Land Model** (Zhu et al., 2019) and the **CESM Community Land Model** (Lawrence et al., 2019)
- **Models are scored** based on statistical comparisons and functional response metrics

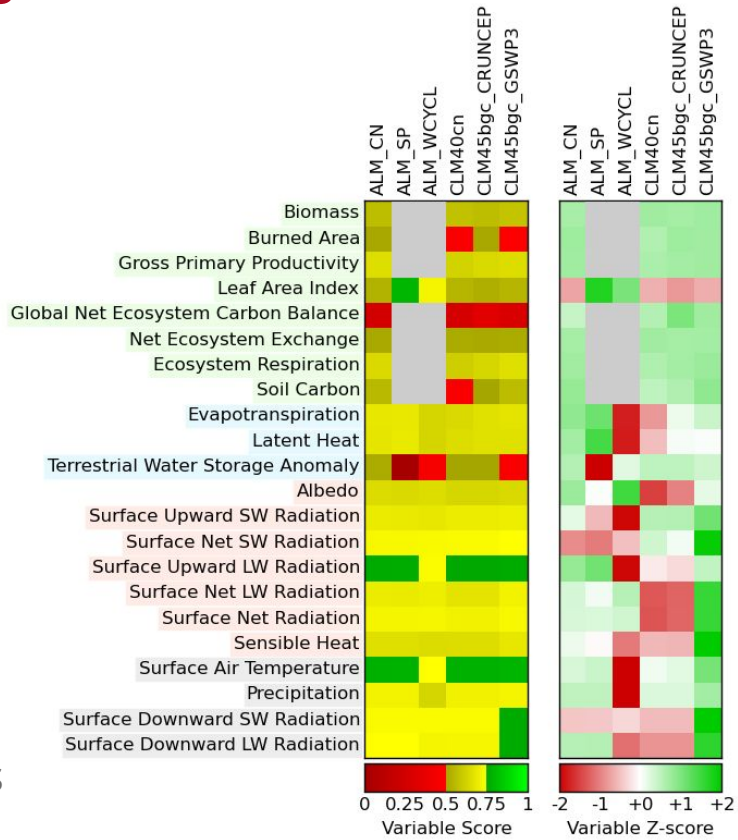

ILAMB Produces Diagnostics and Scores Models

- ILAMB generates a top-level **portrait plot** of models scores
- For every variable and dataset, ILAMB can automatically produce
  - **Tables** containing individual metrics and metric scores (when relevant to the data), including
    - Benchmark and model **period mean**
    - **Bias** and **bias score** (S_{bias})
    - **Root-mean-square error (RMSE)** and **RMSE score** (S_{rmse})
    - **Phase shift** and **seasonal cycle score** (S_{phase})
    - **Interannual coefficient of variation** and **IAV score** (S_{iav})
    - **Spatial distribution score** (S_{dist})
    - **Overall score** (S_{overall}) $\longrightarrow$ $S_{\text{overall}} = \dfrac{S_{\text{bias}} + 2S_{\text{rmse}} + S_{\text{phase}} + S_{\text{iav}} + S_{\text{dist}}}{1+2+1+1+1}$
  - **Graphical diagnostics**
    - Spatial contour maps
    - Time series line plots
    - Spatial Taylor diagrams (Taylor, 2001)
- Similar **tables** and **graphical diagnostics** for functional relationships

ILAMBv2.6 Package Current Variables

- **Biogeochemistry:** Biomass (Contiguous US, Pan Tropical Forest), Burned area (GFED3), CO_2 (NOAA GMD, Mauna Loa), Gross primary production (Fluxnet, GBAF), Leaf area index (AVHRR, MODIS), Global net ecosystem carbon balance (GCP, Khatiwala/Hoffman), Net ecosystem exchange (Fluxnet, GBAF), Ecosystem Respiration (Fluxnet, GBAF), Soil C (HWSD, NCSCDv22, Koven)
- **Hydrology:** Evapotranspiration (GLEAM, MODIS), Evaporative fraction (GBAF), Latent heat (Fluxnet, GBAF, DOLCE), Runoff (Dai, LORA), Sensible heat (Fluxnet, GBAF), Terrestrial water storage anomaly (GRACE), Permafrost (NSIDC)
- **Energy:** Albedo (CERES, GEWEX.SRB), Surface upward and net SW/LW radiation (CERES, GEWEX.SRB, WRMC.BSRN), Surface net radiation (CERES, Fluxnet, GEWEX.SRB, WRMC.BSRN)
- **Forcing:** Surface air temperature (CRU, Fluxnet), Diurnal max/min/range temperature (CRU), Precipitation (CMAP, Fluxnet, GPCC, GPCP2), Surface relative humidity (ERA), Surface down SW/LW radiation (CERES, Fluxnet, GEWEX.SRB, WRMC.BSRN)

CMIP5 vs. CMIP6 Models

- The CMIP6 suite of land models (right) has improved over the CMIP5 suite of land models (left)
- The multi-model mean outperforms any single model for each suite of models
- The multi-model mean CMIP6 land model is the “best model” overall
- Why did CMIP6 land models improve?

(Hoffman et al., in prep)

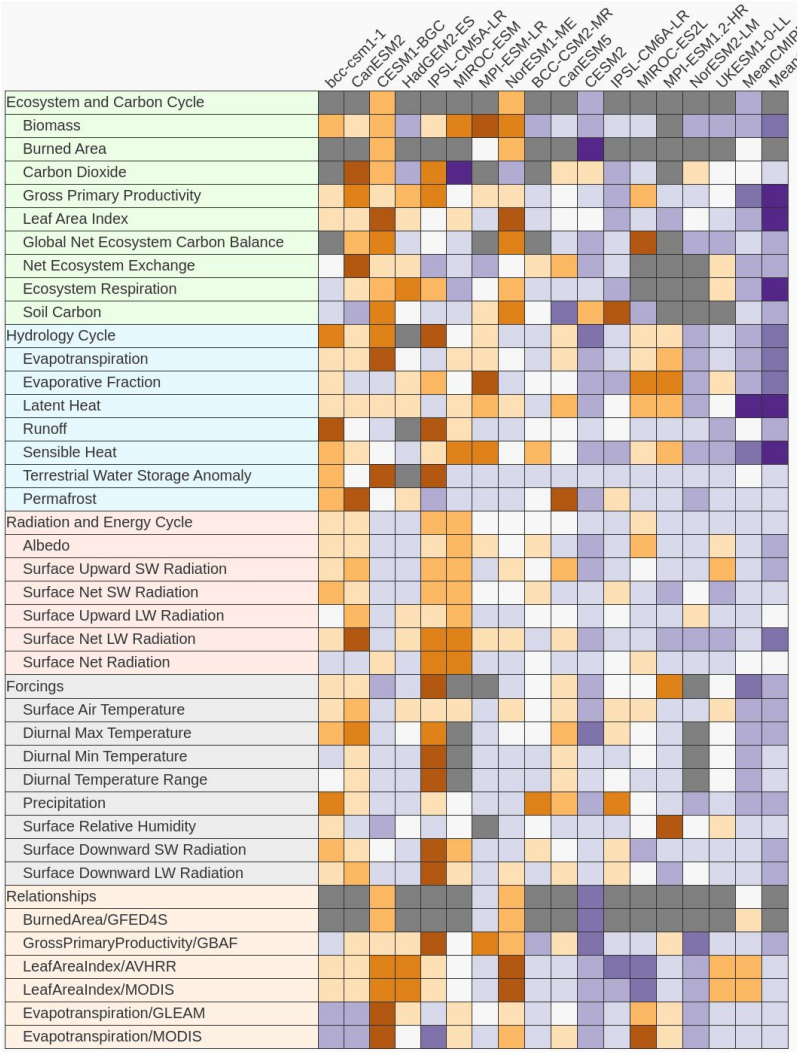

bcc-csm1-1

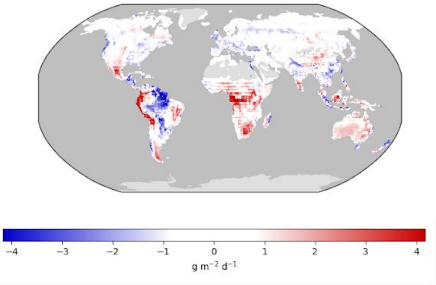

BCC-CSM2-MR

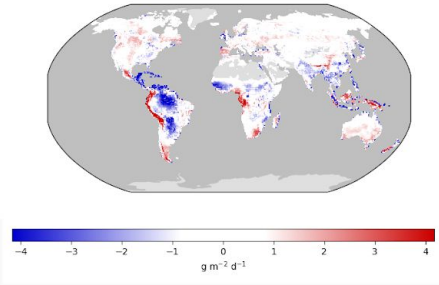

CanESM2

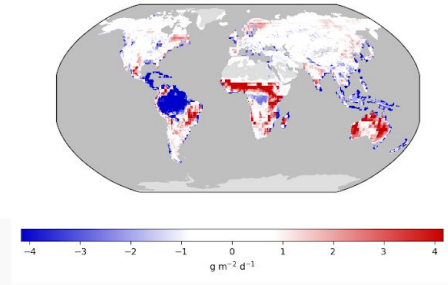

CanESM5

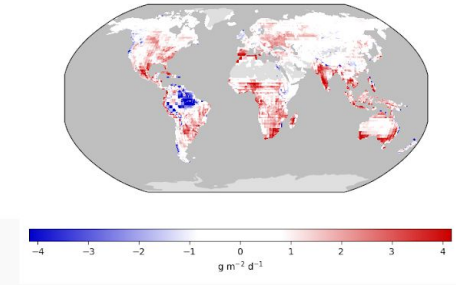

CESM1-BGC

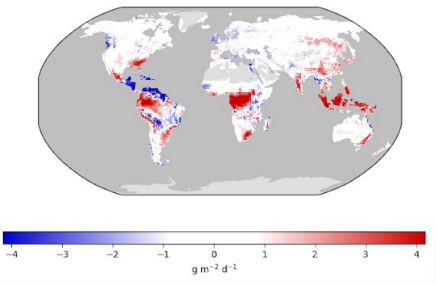

CESM2

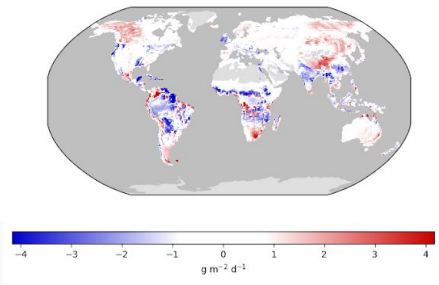

GFDL-ESM2G

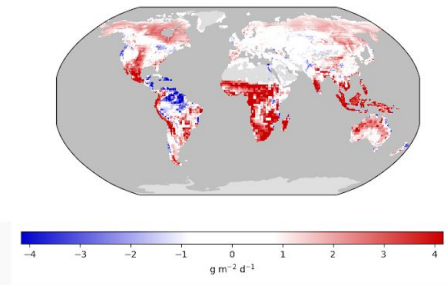

GFDL-ESM4

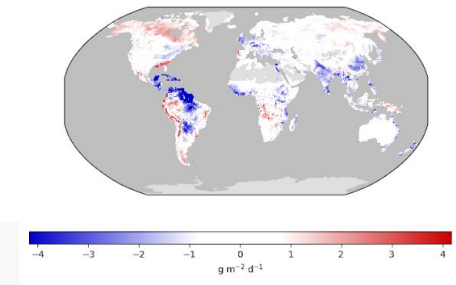

IPSL-CM5A-LR

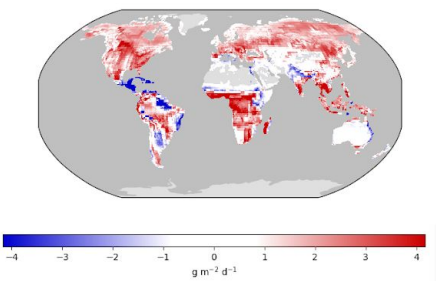

IPSL-CM6A-LR

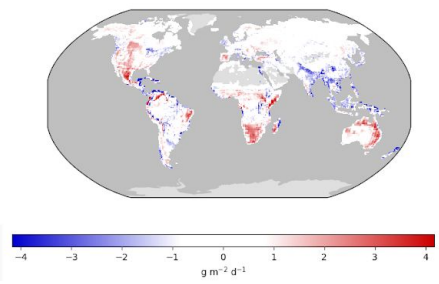

MeanCMIP5

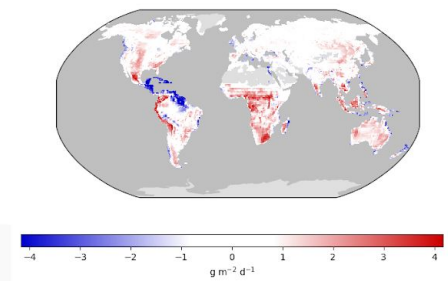

MeanCMIP6

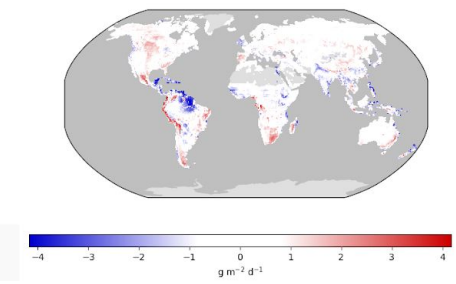

Gross Primary Productivity

	Download Data	Period Mean (original grids) [Pg yr-1]	Model Period Mean (intersection) [Pg yr-1]	Benchmark Period Mean (intersection) [Pg yr-1]	Model Period Mean (complement) [Pg yr-1]	Benchmark Period Mean (complement) [Pg yr-1]	Bias [g m-2 d-1]	RMSE [g m-2 d-1]	Phase Shift [months]	Bias Score [1]	RMSE Score [1]	Seasonal Cycle Score [1]	Spatial Distribution Score [1]	Overall Score [1]
Benchmark	[-]	114.												
bcc-csm1-1	[-]	123.	112.	114.	8.79	0.0945	0.238	1.51	1.01	0.484	0.435	0.830	0.955	0.628
BCC-CSM2-MR	[-]	114.	107.	113.	5.88	0.671	-0.0233	1.52	1.11	0.479	0.447	0.817	0.941	0.626
CanESM2	[-]	129.	117.	114.	9.54		0.0601	2.31	2.00	0.388	0.437	0.850	0.838	0.549
CanESM5	[-]	141.	128.	114.	10.1		0.730	1.87	1.60	0.449	0.418	0.710	0.948	0.589
CESM1-BGC	[-]	129.	123.	113.	5.55	0.660	0.379	1.66	1.20	0.426	0.468	0.765	0.889	0.603
CESM2	[-]	110.	104.	113.	5.57	0.642	-0.0542	1.62	1.32	0.458	0.466	0.774	0.933	0.619
GFDL-ESM2G	[-]	167.	152.	114.	12.4		1.26	2.78	1.38	0.377	0.238	0.735	0.897	0.517
GFDL-ESM4	[-]	105.	99.0	114.	6.18		-0.177	1.59	1.49	0.495	0.403	0.702	0.939	0.588
IPSL-CM5A-LR	[-]	165.	150.	113.	11.7	0.515	1.18	2.68	1.20	0.327	0.352	0.781	0.896	0.542
IPSL-CM6A-LR	[-]	115.	109.	113.	5.27	0.708	0.111	1.39	1.14	0.547	0.477	0.790	0.961	0.650
MeanCMIP5	[-]	121.	115.	114.	6.65		0.574	1.41	0.981	0.494	0.502	0.799	0.965	0.652
MeanCMIP6	[-]	116.	110.	114.	6.26		0.129	1.17	0.931	0.572	0.522	0.826	0.956	0.679
MIROC-ESM	[-]	129.	118.	102.	9.04	11.4	0.396	1.90	1.27	0.463	0.435	0.767	0.920	0.604
MIROC-ESM2L	[-]	116.	104.	113.	9.90	0.119	-0.0111	1.95	1.99	0.409	0.379	0.823	0.920	0.543
MPI-ESM-LR	[-]	169.	159.	104.	8.91	9.81	1.36	2.36	1.29	0.402	0.371	0.715	0.930	0.558
MPI-ESM1.2-LR	[-]	141.	133.	104.	6.89	9.81	0.725	2.06	1.13	0.409	0.393	0.769	0.925	0.578
NorESM1-ME	[-]	129.	120.	114.	7.82		0.386	1.86	1.25	0.387	0.456	0.761	0.856	0.583
NorESM2-LM	[-]	107.	97.5	114.	7.59		-0.0828	1.63	1.31	0.443	0.472	0.791	0.938	0.623
UK-HadGEM2-ES	[-]	137.	130.	113.	6.93	0.848	0.602	2.01	1.10	0.389	0.388	0.820	0.855	0.568
UKESM1-0-LL	[-]	126.	119.	113.	7.06	0.825	0.387	1.77	1.16	0.436	0.419	0.791	0.924	0.598

- Multimodel GPP is compared with global seasonal GBAF estimates
- We can see Improvements across generations of models (e.g., CESM1 vs. CESM2, IPSL-CM5A vs. 6A)
- The mean CMIP6 and CMIP5 models perform best

Spatial Taylor Diagram

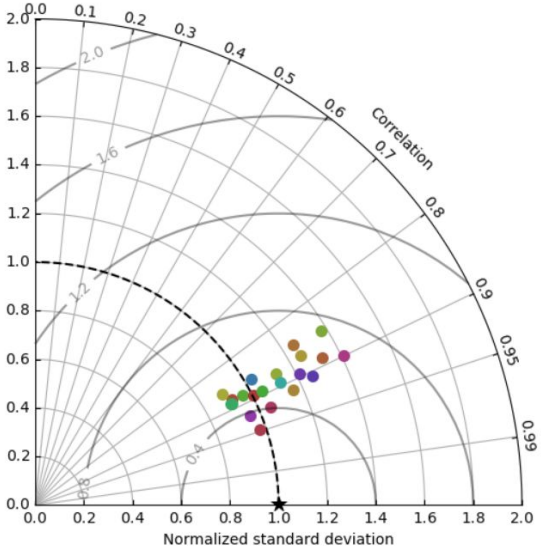

Argonne NATIONAL LABORATORY · BROOKHAVEN NATIONAL LABORATORY · Berkeley Lab · Los Alamos NATIONAL LABORATORY · NCAR NATIONAL CENTER FOR ATMOSPHERIC RESEARCH · OAK RIDGE National Laboratory · UCI · MICHIGAN

Precipitation/GPCPv2.3

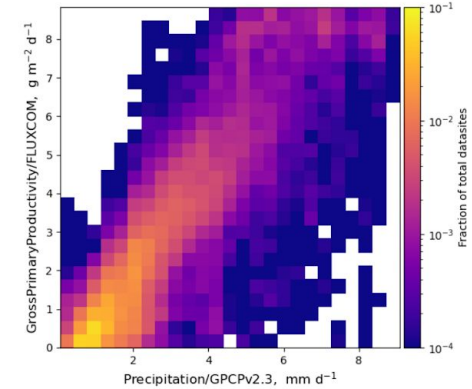

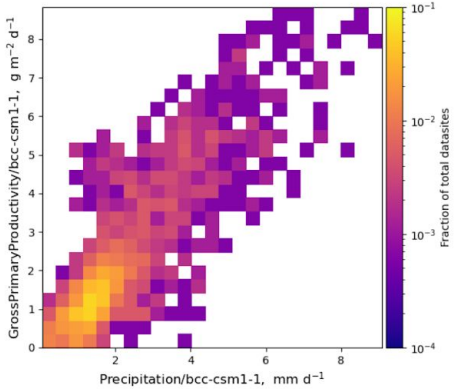

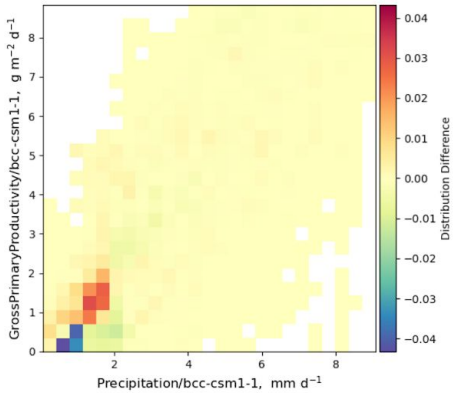

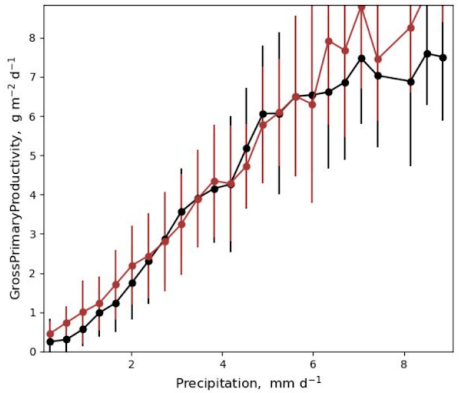

SurfaceDownwardSWRadiation/CERESed4.1

SurfaceNetSWRadiation/CERESed4.1

SurfaceAirTemperature/CRU4.02

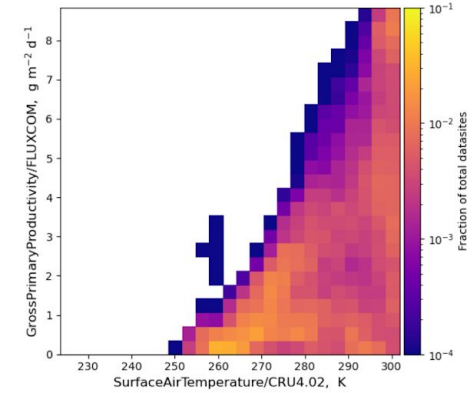

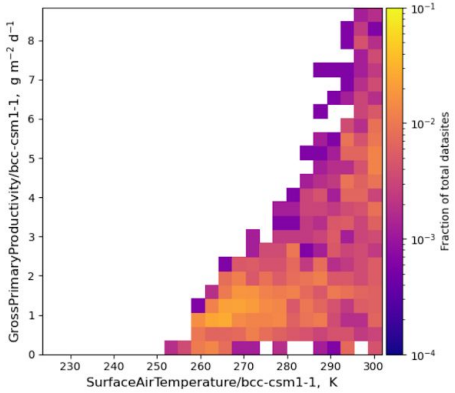

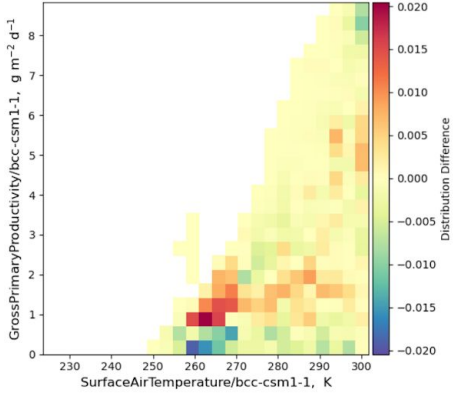

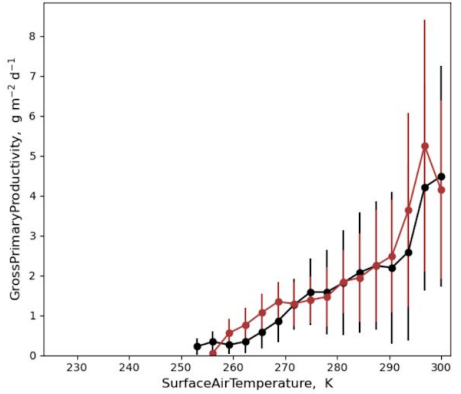

Reasons for Land Model Improvements

ESM improvements in climate forcings (temperature, precipitation, radiation) likely partially drove improvements exhibited by land carbon cycle models

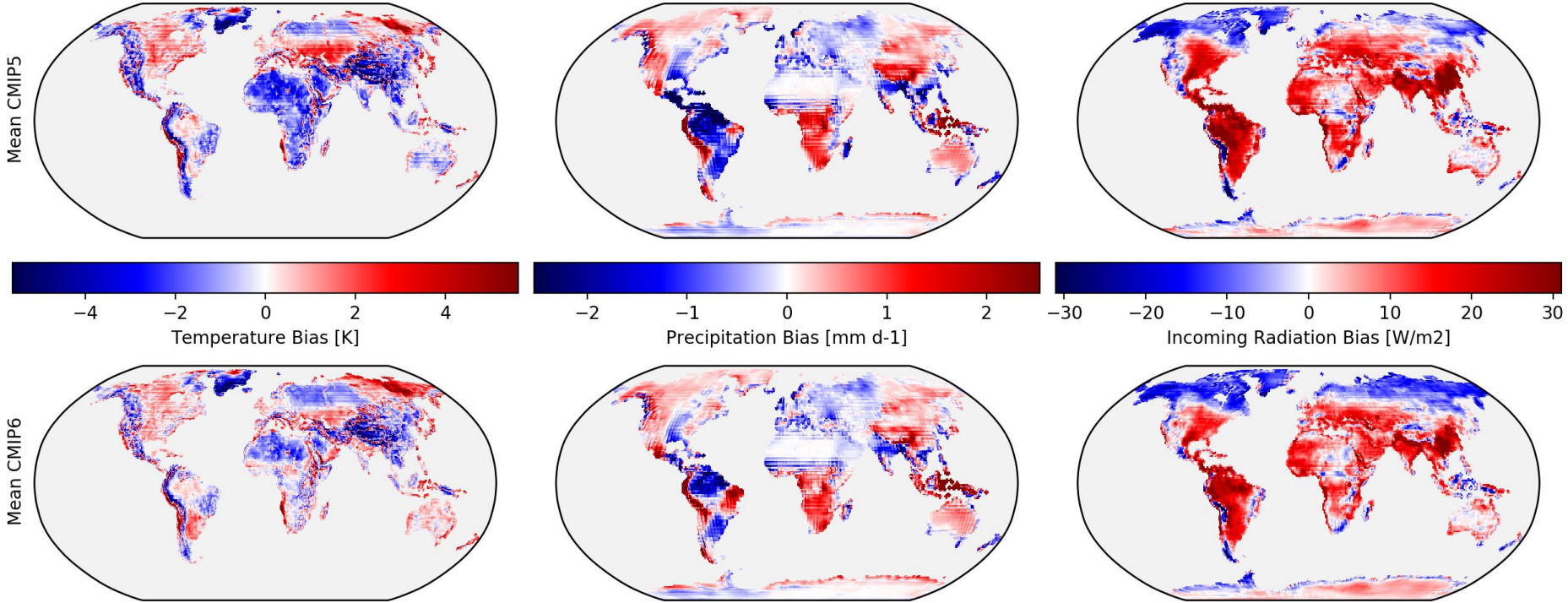

(Hoffman et al., in prep)

Reasons for Land Model Improvements

Differences in bias scores for temperature, precipitation, and incoming radiation were primarily positive, further indicating more realistic climate representation

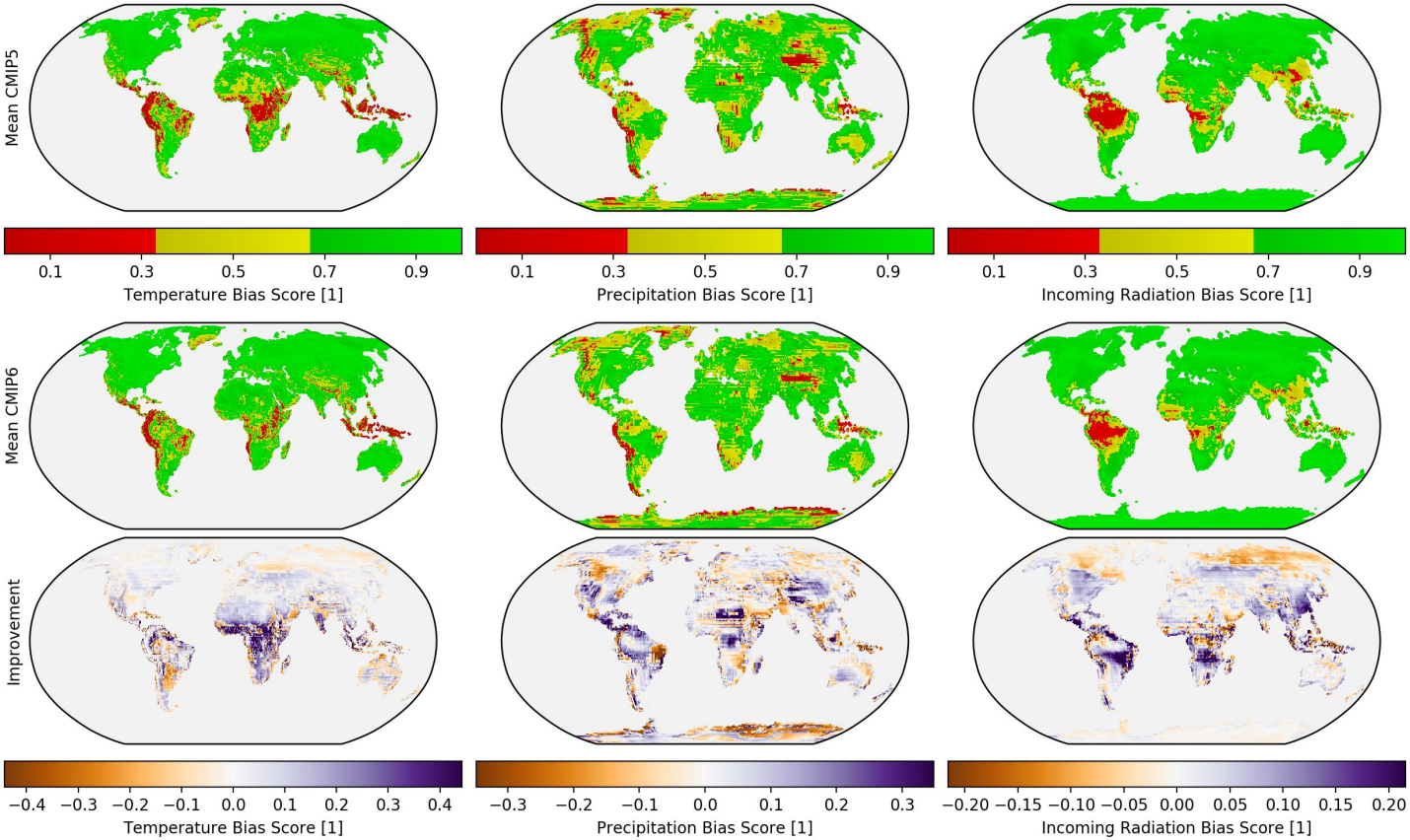

(Hoffman et al., in prep)

Reasons for Land Model Improvements

While forcings got better, the largest improvements were in **variable-to-variable relationships**, suggesting that increased land model complexity was also partially responsible for higher CMIP6 model scores

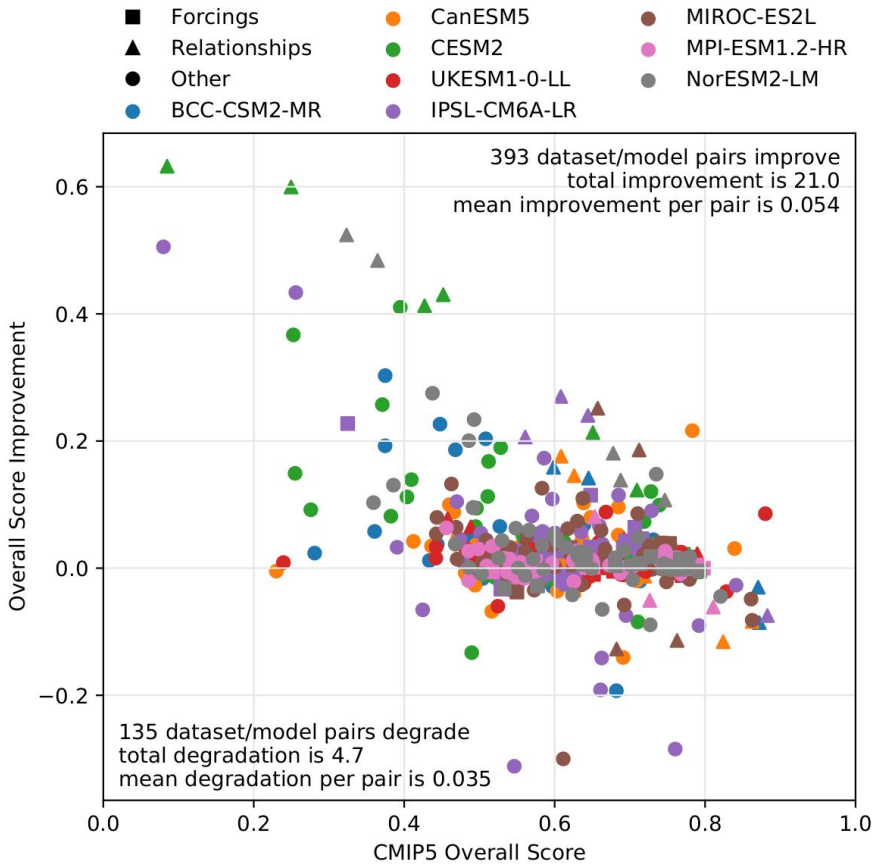

ILAMB & IOMB CMIP5 vs 6 Evaluation

- (a) ILAMB and (b) IOMB have been used to evaluate how land and ocean model performance has changed from CMIP5 to CMIP6
- Model fidelity is assessed through comparison of historical simulations with a wide variety of contemporary observational datasets
- The UN's Intergovernmental Panel on Climate Change (IPCC) Sixth Assessment Report (AR6) from Working Group 1 (WG1) Chapter 5 contains the full ILAMB/IOMB evaluation as Figure 5.22

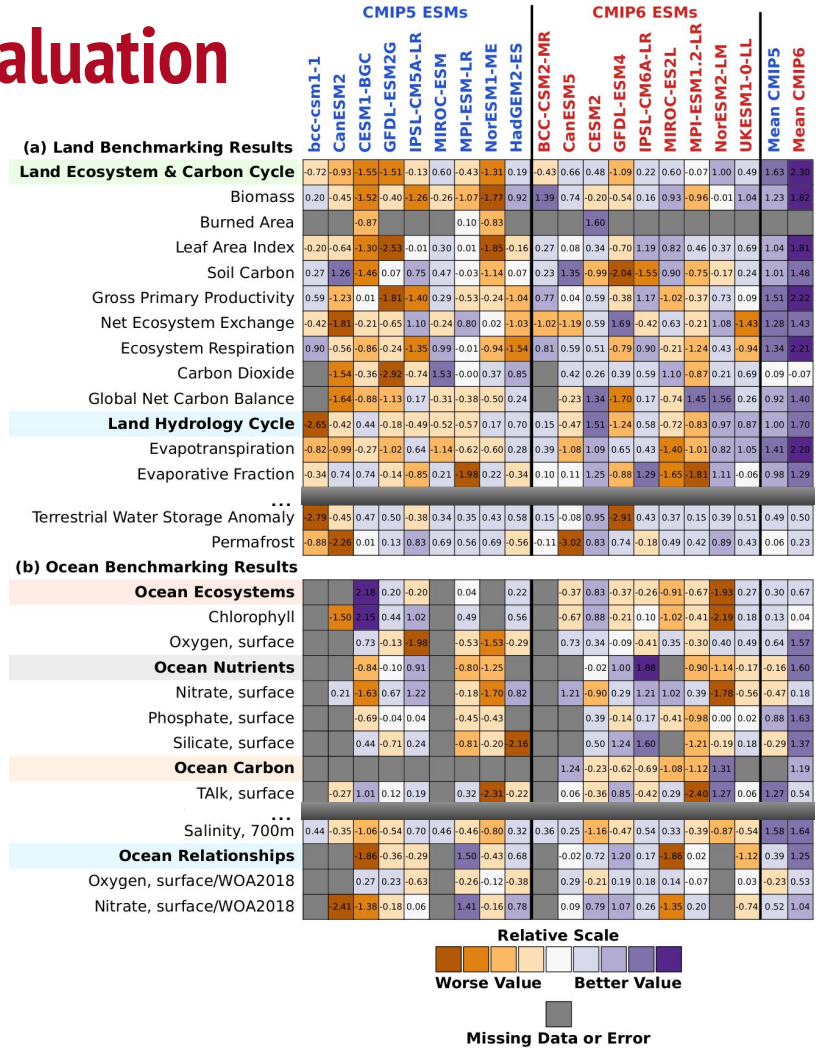

Oak Ridge National Laboratory (ORNL) and the Computational Earth Sciences Group

Frontier *at Oak Ridge National Laboratory is the #2 fastest supercomputer on the [TOP500] List and the first supercomputer to break the exaflop barrier (November 18, 2024).*

Computational Earth Sciences Group

Forrest M. Hoffman
Group Leader

The **Computational Earth Sciences Group (CESG)** improves process understanding of the global Earth system by developing and applying models, machine learning, and computational tools at scale; integrating observational data; and quantifying Earth system predictability and uncertainty associated with interactions between water, energy, biogeochemical cycles, and aerosols.

- Advances predictive understanding and simulation of atmospheric, terrestrial, cryospheric, and marine coupled systems
- Quantifies interactions and feedbacks within and between the Earth system and terrestrial, marine, and subsurface biogeochemical cycles
- Develops and applies methods and tools, including AI and machine learning, for quantitative assessment and benchmarking of coupled, multiscale Earth system models at global and regional scales
- Provides metrics for stakeholders through projects that connect to integrated and vulnerability assessment and adaptation projects

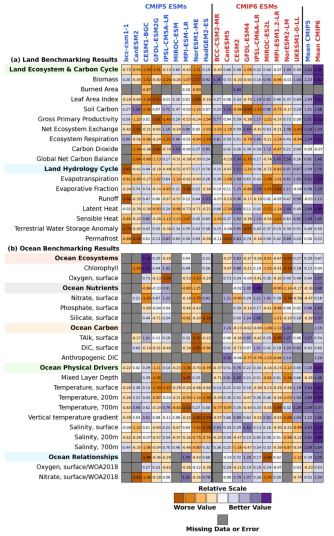

(IPCC AR6 WG1, 2021, Figure 5.22)

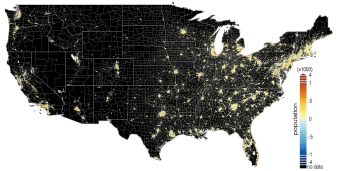

(Batibeniz et al., *Earth's Future*, 2020)

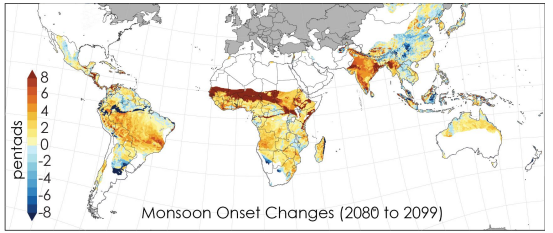

(Ashfaq et al., *Clim. Dyn.*, 2020)

Sensitivity of ENSO Teleconnection to Extremes: Model Resolution and Air-sea Coupling

Objective: Evaluate representation of ENSO teleconnection to precipitation extremes over North America in DOE E3SM historical simulations.

New Science: Extreme value analysis reveals that high resolution models generally improve the simulation of precipitation extremes over North America. However, the improvement in ENSO teleconnection to precipitation extremes is marginal. Model bias over Western North America and Southeastern US is associated with a stronger and more widespread reduction of extratropical cyclone activity during El Nino years than observed. Air-sea coupling enhances this behavior as evident from prescribed SST simulations.

Results/Impacts: The deficiencies in the simulation of ENSO teleconnection to precipitation extremes appears to be due to ENSO associated large scale atmospheric drivers of precipitation extremes. Improving mid-latitude atmosphere-ocean coupled response to ENSO events in models could alleviate these biases.

Mahajan, Salil, Q. Tang, N. Keen, C. Golaz, L. Van-Roekel (2020), Sensitivity of the simulation of ENSO teleconnections to precipitation extremes over North America in an ESM: Model resolution and air-sea coupling, *Journal of Climate (in preparation).*

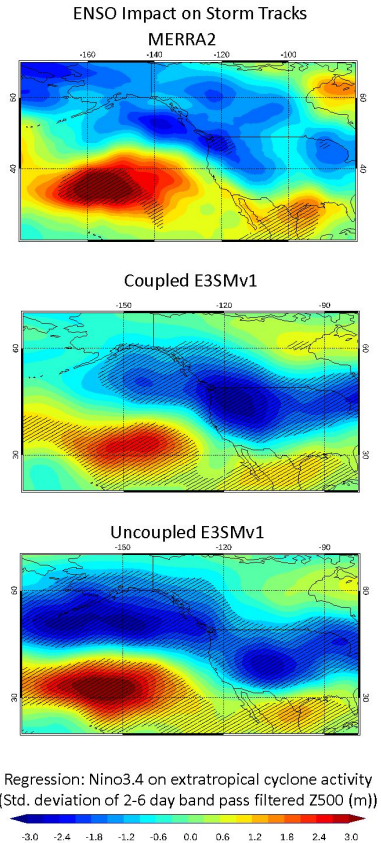

ENSO impacts on extra-tropical cyclone (storm track) activity in MERRA2 reanalysis product (1980-2018), and low-resolution (1-degree) E3SM v1 coupled and prescribed SST (uncoupled) historical ensembles (1979-2015).

Revisiting Recent U.S. Heat Waves in a Warmer and More Humid Climate

Contact: Deeksha Rastogi, E-mail: rastogid@ornl.gov

Objective: Investigate the characteristics of temperature-based (dry) and temperature-humidity-based (humid) temporally compounded heat waves in present and a warmer climate across the United States using a pair of high resolution spectrally nudged numerical model simulations.

New Science:

1) We show that humidity exacerbated the geographical footprint of heat waves more for some years (e.g. higher humidity impacts were identified during 2010 as compared to 2012 over the Southeast).

2) In a warmer climate, dry heat waves are projected to become drier, while humid heat waves remain humid. However, the overall increase in daily maximum temperature intensifies the heat stress during both future humid and dry heat waves across all regions.

Significance: There is a projected increase in apparent (or feels like) temperature and human exposure to extreme heat by the 21st century. This study utilized a set of high-resolution numerical simulations with large-scale circulation constrained, to emphasize the importance of thermodynamic drivers in determining future heat wave characteristics.

Citation - Rastogi, D., Lehner, F., & Ashfaq, M. Revisiting Recent U.S. Heat Waves in a Warmer and More Humid Climate. *Geophysical Research Letters*, 47, e2019GL086736, **https://doi.org/10.1029/2019GL086736**

Humid versus Dry Heat Wave Characteristics over the Southeast U.S. during 2010 and 2012 Summers

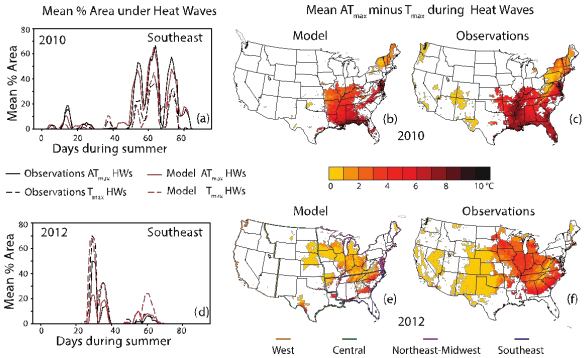

Figure: Daily maximum temperature (T_{max}) and daily maximum apparent temperature (AT_{max}) heatwaves during 2010 and 2012 summer over the southeast United States. Line plots show mean percentage area under heatwaves over the Southeast United States for summer (June-July-August) during (a) 2010 (d) 2012. Spatial maps show average differences between AT_{max} and T_{max} during the heatwave days in 2010 for (b) model (WRF) and (l) observations (PRISM) and 2012 for (m) model and (n) observations.

Funding:

Energy Exascale Earth System Model (E3SM), US DOE, Office of Science, Office of Biological and Environmental Research (BER)

Advance Study Program fellowship awarded by Graduate Visitor Program at National Center for Atmospheric Research (NCAR).

Support for data storage and analysis is provided by Computational Information Systems Laboratory at National Center for Atmospheric Research, Boulder, CO.

CLIMATE CHANGE SCIENCE INSTITUTE
OAK RIDGE NATIONAL LABORATORY

Advancing a predictive understanding of large-scale earth systems through machine learning

Objective	•Use limited expensive earth system model simulation data to build a fast-to-evaluate surrogate model for accurate predictions in large-scale earth systems.
New science	•Advanced singular value decomposition method has been developed to produce a simple neural network (NN) surrogate model which greatly reduces the number of required training data. •Efficient Bayesian optimization algorithm has been developed to generate an accurate NN surrogate.
Significance	•An accurate and fast-to-evaluate surrogate enables efficient model-data integration in earth system modeling. •Advanced application of machine learning techniques for Earth and environmental systems sciences.

Lu, D. and D. Ricciuto, Efficient surrogate modeling methods for large-scale Earth system models based on machine learning techniques. https://doi.org/10.5194/gmd-2018-327

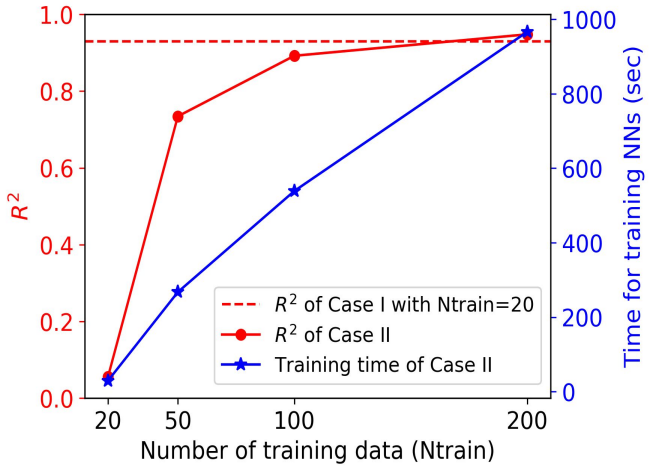

The resulted simple and optimized NN enables only 20 training data to produce accurate predictions of regional GPPs otherwise 200 data are needed for the similar accuracy.

Monsoon seasons will shift and shrink at the higher levels of radiative forcing

Objective: Quantification of future changes in the global monsoons at various levels of radiative forcing.

New Science:

- For the first time, a global view of changes in monsoon characteristics using an unprecedented ensemble of high-resolution regional climate model experiments for two different radiative forcing scenarios.
- A spatially robust delay in the start of global monsoons and shrinking of monsoon seasons at higher levels of radiative forcing.
- Deeper boundary layer and reduced atmospheric saturation during pre-monsoons suppress convective precipitation, which weakens atmospheric diabatic heating and delays the transitioning of monsoon regions into deep convective states.
- No significant changes in monsoons at lower radiative forcing levels.

Significance: Two-thirds of global population relies on monsoons precipitation. Projected changes in the global monsoons will impact energy, health, agricultural and water resource sectors and has the potential to disrupt global economic supply chains. The possibility that a major change in global monsoons can be avoided at lower levels of radiative forcing highlights the urgent need for steps towards emissions stabilization.

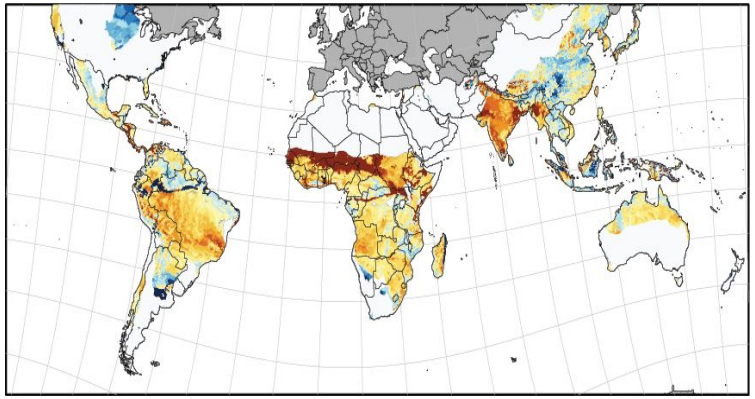

Delay in the start of global monsoons at higher radiative forcing levels

Part of the climate model simulations, analyses, and data storage were supported by the OLCF resources.

Ashfaq, Moetasim, T. Cavazos, M. S. Reboita, J. A. Torres-Alavez, E.-S. Im, C. F. Olusegun, L. Alves, **Kesondra Key**, M. O. Adeniyi, M. Tall, M. Bamba Sylla, **Shahid Mehmood**, Q. Zafar, S. Das, I. Diallo, E. Coppola, and F. Giorgi (2020), Robust late twenty-first century shift in the regional monsoons in RegCM-CORDEX simulations, *Clim. Dyn.*, doi:10.1007/s00382-020-05306-2.

The Earth Has Humans, So Why Don't Our Climate Models?

Objective: To inspire an interdisciplinary effort to couple models of human behavior and social systems with climate models to overcome deficiencies in representing feedbacks.
Approach: A multi-model approach that considers a range of theories and representations of human perception and behavior, driven by a suite of social factors, is proposed.
Results/Impacts: We describe the importance of linking social factors with climate processes and identify four priorities for advancing the development of coupled social-climate models: 1) evaluate an array of behavioral theories, 2) identify regional climate impacts on humans, 3) incorporate influence of diverse social systems, and 4) improve representation of how perceptions and behavior influence greenhouse gas emissions.

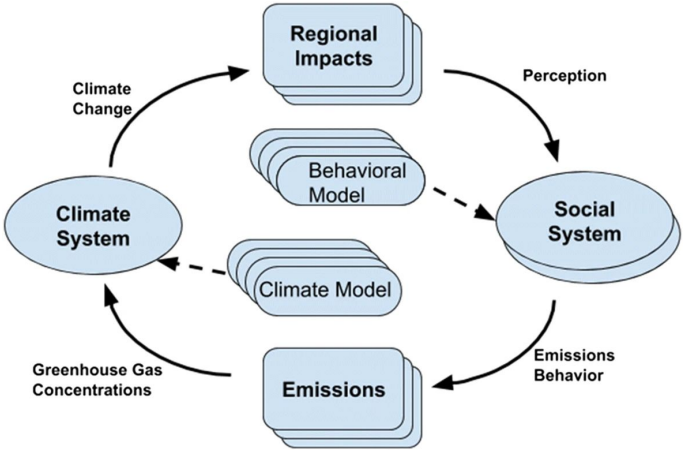

Figure: Schematic diagram demonstrating a strategy for coupling social models with climate models.

Beckage, B., K. Lacasse, J. M. Winter, L. J. Gross, N. Fefferman, **Forrest M. Hoffman**, S. S. Metcalf, T. Franck, E. Carr, A. Zia, and A. Kinzig (2020), The Earth Has Humans, So Why Don't Our Climate Models? *Clim. Change*, doi:10.1007/s10584-020-02897-x.

A Semi-implicit Barotropic Mode Solver for the E3SM Ocean Model Enables Faster and More Stable Ocean Simulations

Objective: To solve the barotropic mode in the E3SM ocean model more efficiently and stably as a competitor of an existing scheme.

Approach: Implement the semi-implicit method for the barotropic mode using a more scalable iterative method with an optimized preconditioner.

Results/Impacts: Several numerical experiments demonstrate that the semi-implicit barotropic mode solver has almost the same accuracy and better parallel scalability compared with the existing scheme while allowing faster and more stable simulations. The semi-implicit solver accelerates the barotropic mode up to 2.9 faster than the existing scheme on 16,320 processors. In addition, this semi-implicit solver provides a more flexible choice of a time step size to model users.

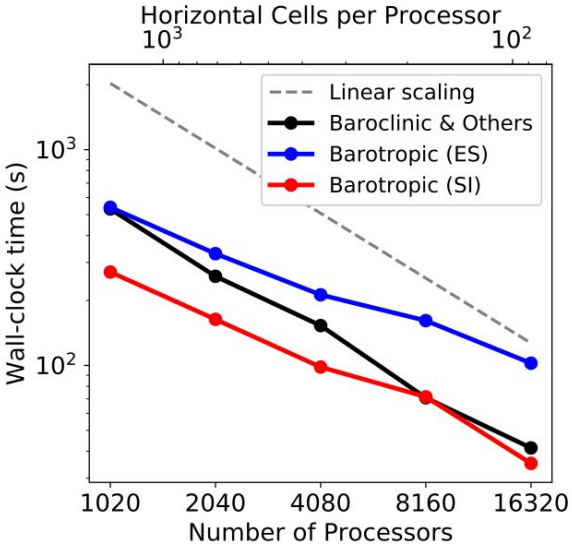

Figure: Strong scaling results for the barotropic mode solved by the explicit-subcycling scheme (ES, the existing scheme) and the semi-implicit method (SI). The MPAS-O model was run on the National Energy Research Scientific Computing Center's Cori supercomputer.

Kang, H.-G., **K. J. Evans**, M. R. Petersen, and P. W. Jones (2020), A scalable barotropic mode solver for the MPAS-Ocean, *J. Adv. Model Earth Sy.*, in preparation.

OAK RIDGE National Laboratory · Los Alamos NATIONAL LABORATORY · E3SM Energy Exascale Earth System Model

Geoengineering Increases the Global Land Carbon Sink

Objective: To examine stratospheric aerosol intervention (SAI) impacts on plant productivity and terrestrial biogeochemistry.

Approach: Analyze and compare simulation results from the Stratospheric Aerosol Geoengineering Large Ensemble (GLENS) project from 2010 to 2097 under RCP8.5 with and without SAI.

Results/Impacts: In this scenario, SAI causes terrestrial ecosystems to store an additional 79 Pg C globally as a result of lower ecosystem respiration and diminished disturbance effects by the end of the 21st century, yielding as much as a 4% reduction in atmospheric CO_2 mole fraction that progressively reduces the SAI effort required to stabilize surface temperature.

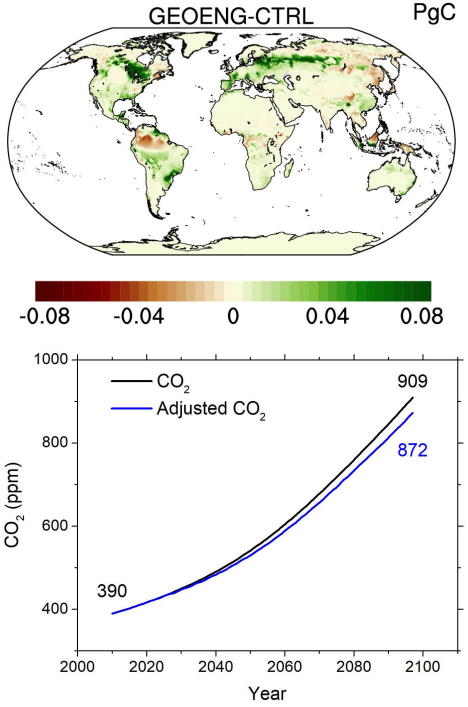

Figure: The larger sink under SAI increased land C storage by 79 Pg C by 2097, which would reduce the projected atmospheric CO_2 level.

Yang, C.-E., **F. M. Hoffman**, D. M. Ricciuto, S. Tilmes, L. Xia, D. G. MacMartin, B. Kravitz, J. H. Richter, M. Mills, and J. S. Fu (2020), Assessing Terrestrial Biogeochemical Feedbacks in a Strategically Geoengineered Climate, *Environ. Res. Lett.*, doi:10.1088/1748-9326/abacf7.

University of Tennessee and the Bredesen Center

University of Tennessee, Knoxville

The Bredesen Center

The Bredesen Center for Interdisciplinary Research and Graduate Education unites resources and capabilities from the University of Tennessee and Oak Ridge National Laboratory to promote advanced research and to provide innovative solutions to global challenges in energy, engineering, and computation under the umbrella of the UT-Oak Ridge Innovation Institute (UT-ORII).

Seeking to create opportunities for exceptional students to engage in interdisciplinary research and education, the Bredesen Center offers a doctoral degree in the following areas:

- Energy Science and Engineering (ESE)
- Data Science and Engineering (DSE)

THE UNIVERSITY OF TENNESSEE

Oak Ridge Innovation Institute

Leadership PhD Programs:
- Energy Science & Engineering
- Data Science & Engineering
- Genome Science & Technology

Project Areas Include:
- Quantum Information Science & Autonomous Systems
- Energy Storage
- Materials & Manufacturing
- Predictive Biology

Length and Cost:
- Tuition-waiver, Insurance, Stipend
- Graduate Assistantship
- Estimated Completion in 4-6 years

Interdisciplinary Aspects:
- Research at ORNL
- Customizable Curriculum
- Knowledge Breadth Courses
- Team Science

More Info (ESE/DSE): https://bredesencenter.utk.edu **(GST):** https://gst.tennessee.edu/

Timothy Guthrie | tguthrie@utk.edu | 865-974-1088

Questions?

References (1/2)

Bonan, G. B., D. L. Lombardozzi, W. R. Wieder, K. W. Oleson, D. M. Lawrence, F. M. Hoffman, and N. Collier (2019), Model structure and climate data uncertainty in historical simulations of the terrestrial carbon cycle (1850–2014), *Global Biogeochem. Cycles*, 33(10):1310–1326, doi:10.1029/2019GB006175.

Collier, N., F. M. Hoffman, D. M. Lawrence, G. Keppel-Aleks, C. D. Koven, W. J. Riley, M. Mu, and J. T. Randerson (2018), The International Land Model Benchmarking (ILAMB) system: Design, theory, and implementation, *J. Adv. Model. Earth Syst.*, 10(11):2731–2754, doi:10.1029/2018MS001354.

Eyring, V., P. M. Cox, G. M. Flato, P. J. Gleckler, G. Abramowitz, P. Caldwell, W. D. Collins, B. K. Gier, A. D. Hall, F. M. Hoffman, G. C. Hurtt, A. Jahn, C. D. Jones, S. A. Klein, J. Krasting, L. Kwiatkowski, R. Lorenz, E. Maloney, G. A. Meehl, A. Pendergrass, R. Pincus, A. C. Ruane, J. L. Russell, B. M. Sanderson, B. D. Santer, S. C. Sherwood, I. R. Simpson, R. J. Stouffer, and M. S. Williamson (2019), Taking climate model evaluation to the next level, *Nat. Clim. Change*, 9(2):102–110, doi:10.1038/s41558-018-0355-y.

Hoffman, F. M., C. D. Koven, G. Keppel-Aleks, D. M. Lawrence, W. J. Riley, J. T. Randerson, A. Ahlström, G. Abramowitz, D. D. Baldocchi, M. J. Best, B. Bond-Lamberty, M. G. De Kauwe, A. S. Denning, A. R. Desai, V. Eyring, J. B. Fisher, R. A. Fisher, P. J. Gleckler, M. Huang, G. Hugelius, A. K. Jain, N. Y. Kiang, H. Kim, R. D. Koster, S. V. Kumar, H. Li, Y. Luo, J. Mao, N. G. McDowell, U. Mishra, P. R. Moorcroft, G. S. H. Pau, D. M. Ricciuto, K. Schaefer, C. R. Schwalm, S. P. Serbin, E. Shevliakova, A. G. Slater, J. Tang, M. Williams, J. Xia, C. Xu, R. Joseph, and D. Koch (2017), *International Land Model Benchmarking (ILAMB) 2016 Workshop Report*, Technical Report DOE/SC-0186, U.S. Department of Energy, Office of Science, Germantown, Maryland, USA, doi:10.2172/1330803.

References (2/2)

Lawrence, D. M., R. A. Fisher, C. D. Koven, K. W. Oleson, S. C. Swenson, G. B. Bonan, N. Collier, B. Ghimire, L. van Kampenhout, D. Kennedy, E. Kluzek, P. J. Lawrence, F. Li, H. Li, D. Lombardozzi, W. J. Riley, W. J. Sacks, M. Shi, M. Vertenstein, W. R. Wieder, C. Xu, A. A. Ali, A. M. Badger, G. Bisht, M. van den Broeke, M. A. Brunke, S. P. Burns, J. Buzan, M. Clark, A. Craig, K. Dahlin, B. Drewniak, J. B. Fisher, M. Flanner, A. M. Fox, P. Gentine, F. M. Hoffman, G. Keppel-Aleks, R. Knox, S. Kumar, J. Lenaerts, L. R. Leung, W. H. Lipscomb, Y. Lu, A. Pandey, J. D. Pelletier, J. Perket, J. T. Randerson, D. M. Ricciuto, B. M. Sanderson, A. Slater, Z. M. Subin, J. Tang, R. Q. Thomas, M. V. Martin, and X. Zeng (2019), The Community Land Model Version 5: Description of new features, benchmarking, and impact of forcing uncertainty, *J. Adv. Model. Earth Syst.*, 11(12):4245–4287, doi:10.1029/2018MS001583.

Zhu, Q., W. J. Riley, J. Tang, N. Collier, F. M. Hoffman, X. Yang, and G. Bisht (2019), Representing nitrogen, phosphorus, and carbon interactions in the E3SM Land Model: Development and global benchmarking, *J. Adv. Model. Earth Syst.*, 11(7):2238–2258, doi:10.1029/2018MS001571.